Published OnlineFirst November 6, 2013; DOI: 10.1158/0008-5472.CAN-13-1545

Cancer Research

Doxorubicin Eliminates Myeloid-Derived Suppressor Cells and Enhances the Efficacy of Adoptive T-Cell Transfer in Breast Cancer

Darya Alizadeh, Malika Trad, Neale T. Hanke, et al.

Cancer Res 2014;74:104-118. Published OnlineFirst November 6, 2013.

Published OnlineFirst November 6, 2013; DOI: 10.1158/0008-5472.CAN-13-1545

Microenvironment and Immunology

Cancer Research

Doxorubicin Eliminates Myeloid-Derived Suppressor Cells and Enhances the Efficacy of Adoptive T-Cell Transfer in Breast Cancer

Darya Alizadeh[1,3], Malika Trad[5], Neale T. Hanke[2], Claire B. Larmonier[3], Nona Janikashvili[5], Bernard Bonnotte[5,6], Emmanuel Katsanis[1,2,3,4], and Nicolas Larmonier[1,2,3,4]

Abstract

Myeloid-derived suppressor cells (MDSC) expand in tumor-bearing hosts and play a central role in cancer immune evasion by inhibiting adaptive and innate immunity. They therefore represent a major obstacle for successful cancer immunotherapy. Different strategies have thus been explored to deplete and/or inactivate MDSC *in vivo*. Using a murine mammary cancer model, we demonstrated that doxorubicin selectively eliminates MDSC in the spleen, blood, and tumor beds. Furthermore, residual MDSC from doxorubicin-treated mice exhibited impaired suppressive function. Importantly, the frequency of $CD4^+$ and $CD8^+$ T lymphocytes and consequently the effector lymphocytes or natural killer (NK) to suppressive MDSC ratios were significantly increased following doxorubicin treatment of tumor-bearing mice. In addition, the proportion of NK and cytotoxic T cell (CTL) expressing perforin and granzyme B and of CTL producing IFN-γ was augmented by doxorubicin administration. Of therapeutic relevance, this drug efficiently combined with Th_1 or Th_{17} lymphocytes to suppress tumor development and metastatic disease. MDSC isolated from patients with different types of cancer were also sensitive to doxorubicin-mediated cytotoxicity *in vitro*. These results thus indicate that doxorubicin may be used not only as a direct cytotoxic drug against tumor cells, but also as a potent immunomodulatory agent that selectively impairs MDSC-induced immunosuppression, thereby fostering the efficacy of T-cell–based immunotherapy. *Cancer Res; 74(1); 104–18. ©2013 AACR.*

Introduction

Myeloid-derived suppressor cells (MDSC) have been described as a heterogeneous population of immature myeloid cells that, in different pathological conditions, are impaired in their ability to terminally differentiate into mature myeloid lineages such as macrophages, dendritic cells, or granulocytes (1, 2). MDSC are functionally defined by their capability to inhibit both innate and adaptive immunity. They are potent suppressors of T-cell proliferation and activation in humans and mice (1–4). Phenotypically, mouse MDSC express the markers Gr-1 and CD11b. Two main populations have been described in mice based on the relative expression of 2 epitopes of Gr-1 (Ly6G and/or Ly6C): granulocytic MDSC are $CD11b^+Ly6G^+Ly6C^{low}$, whereas monocytic MDSC are $CD11b^+Ly6G^-Ly6C^{high}$ (5, 6). In human, MDSC are generally identified as $CD14^-$ $CD33^+CD11b^+HLA\text{-}DR^{neg/low}$ cells (6). The immunosuppressive function of MDSC depends on multiple mechanisms, including the production of nitric oxide, peroxynitrites, reactive oxygen species (ROS), and the expression of inducible nitric oxide synthase (iNOS), indoleamine 2,3-dioxygenase (IDO), and/or arginase-1 (5, 7, 8).

A substantial expansion of MDSC in the blood, lymph nodes, bone marrow, and spleen has been detected in multiple mouse cancer models (5, 9). Similarly, accumulation of MDSC has been reported in the blood, lymph nodes, and tumors of patients with various types of cancers, including breast, which correlates with tumor burden and disease stage (10). Tumor-induced MDSC expansion significantly contributes to the mechanisms of cancer-induced immune suppression, and therefore significantly impedes the efficacy of immunotherapeutic approaches (1, 11, 12). Not surprisingly, multiple reports in humans and animal models have indicated that MDSC elimination or inhibition promotes antitumor immunity and enhances the response to immunotherapy (11). Different approaches have thus been explored to target these cells, which include the use of specific antibodies (13), all-*trans* retinoic acid (ATRA; refs. 14–16), or chemotherapeutic molecules such as gemcitabine (17, 18), 5-fluorouracile (5-FU; ref. 19), or docetaxel (20).

Authors' Affiliations: [1]Cancer Biology Graduate Program; [2]Arizona Cancer Center; [3]Department of Pediatrics, College of Medicine; [4]Department of Immunobiology, University of Arizona, Tucson, Arizona; [5]Faculty of Medicine, Dijon, and INSERM UMR 1098, Besancon; and [6]Service de Médecine Interne et Immunologie Clinique, CHU Bocage, Dijon, France

Note: Supplementary data for this article are available at Cancer Research Online (http://cancerres.aacrjournals.org/).

Corresponding Author: Nicolas Larmonier, Department of Pediatrics, University of Arizona, 1501 N. Campbell Avenue, PO Box 245073, Tucson, Arizona 85724-5073. Phone: 520-626-4851; Fax: 520-626-6986; E-mail: nrlarmon@email.arizona.edu

doi: 10.1158/0008-5472.CAN-13-1545

Published OnlineFirst November 6, 2013; DOI: 10.1158/0008-5472.CAN-13-1545

Doxorubicin is an antineoplastic drug broadly used in the treatment of hematological malignancies, soft tissue sarcomas, and several types of carcinomas including breast cancer (21). Extensive evidence has been provided that besides its direct tumoricidal activity, doxorubicin also promotes antitumor immunity (22–26). This drug has indeed been shown to induce an "immunogenic type" of tumor cell death leading to the stimulation of dendritic cell antigen-presenting function (23). Doxorubicin administration has also been reported to enhance the proliferation of tumor-specific $CD8^+$ T cells (27), and to increase the permeability of tumor cells to granzyme B produced by cytotoxic T lymphocytes (CTL; ref. 28). However, whether this drug may impact tumor-induced immunosuppression, specifically by negatively targeting MDSC, remains unclear. In this study, we investigated the effects of doxorubicin on MDSC in the murine breast cancer model 4T1 and explored the possibility of combining this chemotherapeutic drug with immunotherapy. We demonstrated for the first time that doxorubicin eliminated MDSC by triggering apoptosis of these cells. ROS may contribute to doxorubicin-mediated elimination of MDSC. In addition, residual MDSC from doxorubicin-treated mice were impaired in their suppressive function. Of importance, doxorubicin administration led to improved T- and natural killer cell function. The proportion of T- and natural killer (NK) cells expressing perforin and granzyme B was indeed significantly augmented following treatment of tumor-bearing mice with doxorubicin. In addition, doxorubicin increased the proliferation status of T lymphocytes and NK cells. Substantiating these observations, doxorubicin exhibited selective cytotoxic effects on MDSC isolated from patients with cancer. Furthermore, the combination of doxorubicin with T helper (Th) 1 or with recently identified Th_{17} lymphocytes impaired tumor development and metastatic spreading. These findings therefore highlight a novel property of doxorubicin as a potent selective MDSC-targeting agent, which may be used to enhance the efficacy of immunotherapeutic regimens.

Patients and Methods

Patients

A total of $n = 10$ patients with confirmed solid cancers (2 patients with lung, one patient with ovarian, one patient with prostate, one patient with bladder, one patient with colon, one patient with stomach, one patient with kidney, one patient with pancreatic, and one patient with breast cancer) were enrolled in the study before treatment after giving written informed consent in accordance with the Declaration of Helsinki. The study was approved by the Ethic Committee of the University Hospital of Dijon. None of the patients had received chemotherapy or any other immunosuppressive treatment during the previous 3 months.

Animals and tumor cell lines

Six- to eight-week-old Balb/c and C57BL/6 mice were purchased from the National Cancer Institute (NCI). Six- to eight-week-old gp91$^{phox-/-}$ (C57Bl6-Cybb^{tm1Din}) were purchased from Jackson Laboratory. The mice were housed and cared for according to the University of Arizona Institutional Animal and Care Guidelines and Use Committee (IACUC). The 4T1 and EMT6 murine mammary tumor cell lines (Balb/c origin) and the EL4 thymoma cell line (C57BL/6 origin) were obtained from the American Type Culture Collection. 4T1-luc was generated using luciferase reporter plasmid (PGL4-51; InvivoGen). Briefly, the transfection was performed using Fugene6 reagent (Promega) according to the manufacturer's protocol. Stably transfected cells were clonally selected in presence of G418 (800 μg/mL) and luciferase expression was confirmed using the luciferase reporter assay system and a luminometer (Femtomaster FB12; Berthold Detection System), according to the manufacturer's recommendation (Promega).

Bioluminescence imaging

Tumor-bearing animals were injected (i.p.) with D-luciferin (4.29 mg/mouse; Xenogen). Mice were anesthetized using isoflurane (1.5 L/min oxygen, 4% isoflurane) and kept in an induction chamber. Images were captured with an AMI1000 imager (Spectral Instruments Imaging). Light emission was measured over an integration time of 1 minute, 10 minutes after injection of luciferin. Luciferase activity was analyzed using the AMI1000 Software (Spectral Instruments Imaging) to quantify tumor region flux (photons per second) and to assess tumor growth.

Generation of Th_1 and Th_{17}

Naive $CD4^+CD25^-CD62L^+$ T lymphocytes were isolated from the spleen of 6- to 8-week-old Balb/c mice according to the manufacturer's instructions (Miltenyi Biotec). Cells were subsequently cultured at a concentration of 10^6 cells/mL in RPMI 1640 medium supplemented with 10% FBS, 100 U/mL penicillin, 100 μg/mL streptomycin sulfate, 0.5 × MEM non-essential amino acids, and 1 mmol/L sodium pyruvate. Cells were stimulated with anti-CD3– and anti-CD28–coated beads (Invitrogen). Th_1 cells were generated in the presence of interleukin (IL)-12 (10 ng/mL), IL-2 (10 ng/mL), IL-7 (20 ng/mL), and blocking anti-IL-4 antibodies (5 μg/mL; 3-day culture). For the generation of Th_{17} cells, naive T cells were cultured with IL-6 (40 ng/mL), TGF-β (0.5 ng/mL), blocking anti-IFN-γ (5 μg/mL), and anti-IL-4 (5 μg/mL) antibodies for 3 days. Th_{17} cultures were then prolonged in fresh medium containing IL-23 (40 ng/mL) for an additional 3 days. All cytokines were purchased from R&D Systems or Peprotech.

Chemotherapy and chemoimmunotherapy

4T1 or 4T1-Luc cells were injected (1×10^6 cells) orthotopically (mammary fat pad). In some experiments, 7 and 12 days posttumor injection, mice were administered with doxorubicin (2.5 or 5 mg/kg, i.v.), cyclophosphamide (50 mg/kg, i.p.), fludarabine (50 mg/kg, i.p.), melphalan (5 mg/kg, i.p.), vincristine (1 mg/kg, i.v.), etoposide (5 mg/kg, i.p.), or control PBS. Spleens, blood, and tumors were collected 14, 17, and 23 days posttumor cell injection. For evaluating the effects of doxorubicin plus T helper lymphocyte combination therapy, mice were injected with doxorubicin (5 mg/kg) on days 7 and 12 and

Published OnlineFirst November 6, 2013; DOI: 10.1158/0008-5472.CAN-13-1545

with Th_1 or Th_{17} cells (1×10^6 i.v.; 2×10^6 intratumorally) on days 9 and 14 posttumor cell injection. Mice were euthanized for ethical reasons when they exhibited severe morbidity signs because of overwhelming metastatic spreading (endpoint at 4–4.5 weeks) in compliance with IACUC regulations.

MDSC isolation

Spleens were harvested, dissociated, and red blood cells were lysed in lysis buffer (BD Biosciences). MDSC were purified using a mouse MDSC isolation kit according to the manufacturer's instructions (Miltenyi Biotec). The purified cells were used in other experiments.

Flow cytometry analysis

Cell suspensions from blood, spleens, or tumors were filtered and red blood cells were lysed. For extracellular staining, cells were incubated with the indicated combinations of antibodies (CD11b, Ly6C, Ly6G (Gr-1), CD8, CD49b, CD4, CD25, F4/80, CD11c, CCR7, and CD206) or isotype controls (1 hour, 4°C). For intracellular staining, cells were fixed and permeabilized immediately after cell surface staining according to the manufacturer's description (Affymetrix eBioscience). For IFN-γ staining, cells were incubated with a leukocyte stimulating kit (BD Biosciences) for 4 hours. For perforin or granzyme B staining, cells were incubated with anti-CD3– and anti-CD28–coated beads (Invitrogen) and IL-2 (4 ng/mL) for 24 hours. The proliferation status of the cells was assessed by staining with Ki67 according to the manufacturer's protocol (Ki67 detection protocol; BD Biosciences). All antibodies and isotype controls were purchased from BD Biosciences or Affymetrix eBioscience. For the detection of apoptosis, spleen, and blood samples from tumor-bearing mice, untreated or treated with doxorubicin, were dissociated and processed as described earlier. Cells were then stained with Annexin V and propodium iodide (PI), according to the manufacturer's protocol (Apoptosis detection kit; Affymetrix eBioscience). Fluorescence data were collected on a FACSverse or LSRFortessa (BD Biosciences). The data were analyzed using FlowJo software (Tree star Inc.).

Suppression assays

Spleens from naive mice were collected, dissociated, and cells were incubating on nylon wool columns (37°C, 45 minutes) after red blood cell lysis. More than 90% of the eluted cells were T lymphocytes based on T-cell receptor (TCR)αβ expression. These T cells were labeled with 5 mmol/L CellTrace Violet according to the manufacturer's instructions (Invitrogen) and were plated in 96-well plates with anti-CD3– and anti-CD28–coated activation beads (Invitrogen). Isolated MDSC from 4T1 tumor-bearing mice, treated or not with doxorubicin, were then added to the culture (MDSC-to-T-cell ratio = 1:2). After 4 days, cells were harvested, stained with anti-CD4, anti-CD8, and anti-CD25 (Affymetrix eBioscience). Cell proliferation was determined by measuring the dilution of cell trace violet by flow cytometry after gating on the $CD4^+$ or $CD8^+$ cell populations. The proliferation index was determined using the Modfit software (Verity Software House) and percent proliferation was calculated as follows: proliferation (%) = $(T^+ - T) - (S - T)/(T^+ - T) \times 100$, with T^+ is the proliferation index of the control stimulated T cells without MDSC; T is the proliferation index of control nonstimulated T cells without MDSC; and S is the proliferation index of stimulated T cells in the presence of MDSC).

Western blot analysis

Cells were lysed in radioimmunoprecipitation assay buffer and sonicated. Lysates were cleared by centrifugation at 14,000 rpm and protein concentration was determined with the Thermo Scientific BCA protein assay using bovine serum albumin (BSA) as standard. Equal amounts of proteins (30 μg) were separated on 10% or 16% SDS-PAGE gels, transferred onto a polyvinylidene fluoride (PVDF) membrane (Millipore) and probed with primary Abs specific for P-STAT3, STAT3, Arginase-1, IDO, cleaved caspase-3 (Cell Signaling Company), S100A9, S100A8 (R&D Systems), and actin (Sigma-Aldrich) followed by secondary antibody (Jackson ImmunoResearch). Reactive bands were visualized by exposure to film using Super Signal Chemiluminescent Substrate (Thermo Scientific).

ROS detection

Splenocytes from untreated or doxorubicin-treated mice were incubated for 30 minutes with the oxidation-sensitive dye dichlorodihydrofluorescein diacetate (DCFDA; 5 μmol/L; Molecular Probes/Invitrogen). Samples were then labeled with anti-Gr-1 and anti-CD11b antibodies. The level of ROS was detected using flow cytometry as described (29).

Real-time PCR

Cells were collected and total RNA was isolated using TRIzol (Invitrogen). PCR reactions were set up in 96-well plates containing 10 μL 2× IQ Supermix (Bio-Rad), 1 μL TaqMan primer/probe set (ABI), 2 μL of the cDNA synthesis reaction [10% of room temperature (RT) reaction] and 7 μL of nuclease-free water. Reactions were run and analyzed on a Bio-Rad iCycler iQ Real-Time PCR Detection System. Primers for IFN-γ and IL-17 were obtained from Applied Biosystems (Invitrogen).

ELISA

IL-17 and IFN-γ concentration was detected in Th_1- and Th_{17}-cell culture supernatant using ELISA according to the manufacturer's instructions (Affymetrix eBioscience).

Immunofluorescent staining

Tumors and spleens were harvested and frozen. Serial sections (5 μm) were performed from each tissue and mounted. Frozen slides were first fixed in 100% cold methanol for 10 minutes. After blocking for 1 hour at RT [10% normal chicken serum in Tris-buffered saline and 0.1% Tween 20 (TBS-T)/1% BSA] slides were incubated (overnight, 4°C) with anti-Gr-1 (Affymetrix eBioscience; 0.02 mg/mL in TBS-T). Slides were washed with TBS-T and incubated with a secondary chicken anti-rat antibody conjugated with Alexa Fluor 647 for 45 minutes at RT (1:200 in TBST; Invitrogen). Slides

Published OnlineFirst November 6, 2013; DOI: 10.1158/0008-5472.CAN-13-1545

were washed and incubated (2 hours, RT) with a rat anti-mouse CD11b antibody conjugated with FITC (Affymetrix eBioscience; 0.02 mg/mL in TBS-T). Nuclear counterstaining was performed using Sytox orange according to the manufacturer's instructions (Invitrogen). Slides were mounted with fluorescence mounting medium (Dako North America) and visualized using a confocal microscope (Zeiss LSM 510-META NLO).

Statistical analysis

Experiments were performed with 4 to 8 mice per groups as indicated. Mice were individually processed and analyzed separately unless specified otherwise. All analyses were carried out using GraphPad Prism software (GraphPad Software). Analyses were performed by 1- or 2-way ANOVA with a Bonferroni or Dunnett posttest, or a paired t test where appropriate. Statistically significant P values were labeled as follows: ***, $P < 0.001$; **, $P < 0.01$; and *, $P < 0.05$.

Results

Doxorubicin selectively eliminates tumor-induced MDSC in mice bearing established 4T1 mammary tumors

The immunomodulatory effects of doxorubicin have been extensively studied (23, 26). However, the possible impact of this chemotherapeutic agent on suppressive MDSC remains elusive. To address this question, Balb/c mice were injected with 4T1 breast cancer cells and treated with doxorubicin (2.5 and 5 mg/kg; noncurative doses), 7 and 12 days post-tumor implantation (Fig. 1A). We first confirmed that 4T1 tumor growth is associated with substantial MDSC expansion and determined the basal proportion of MDSC in the absence of doxorubicin therapy at different time points following injection of tumor cells (Supplementary Fig. S1; refs. 30 and 31). Doxorubicin significantly reduced the proportion and absolute number of 4T1 tumor-induced MDSC in the spleen (Fig. 1B and C) and blood (Fig. 1D) of treated animals. It is noteworthy that although doxorubicin-mediated elimination of MDSC was prominent on day 14 and 17 posttumor cell injection, these cells were reconstituted by day 23. These results were further confirmed by confocal microscopy analysis of spleen sections (Fig. 1E). Furthermore, MDSC were also depleted within the tumor beds in mice treated with doxorubicin (Supplementary Figs. S2A–S2C). 4T1 tumor development is primarily associated with the expansion of granulocytic MDSC (30, 32). Our results indicate that doxorubicin did not significantly affect monocytic MDSC, which were low in frequency even in untreated animals, but significantly depleted granulocytic MDSC (Supplementary Fig. S2D). These results thus demonstrate that doxorubicin induced elimination of tumor-induced MDSC.

Doxorubicin minimally affects effector immune cell populations

To optimally promote antitumor immunity, immunomodulatory drugs should negatively target immunosuppressive cells while sparing immune effectors. We therefore sought to investigate whether doxorubicin may affect other immune cells, specifically antitumoral effector T lymphocytes and natural killer cells. Interestingly, the proportion of $CD4^+$ and $CD8^+$ T lymphocytes was significantly increased in the spleen and blood of doxorubicin-treated mice (Fig. 2A and B). NK frequency increased in the blood and was not altered in the spleen of the treated animals (Fig. 2C). Consistent with these results, the proliferation status of $CD4^+$ and $CD8^+$ T cells was augmented in doxorubicin-treated animals (Fig. 2D). This preferential targeting of MDSC resulted in a significant increase in the ratios of effector $CD8^+$ T, $CD4^+$ T, or NK cells to suppressive MDSC (Supplementary Fig. S3A). Importantly, the proportion of NK cells and $CD8^+$ T lymphocytes expressing perforin and granzyme B was significantly increased in doxorubicin-treated 4T1 tumor-bearing mice (Fig. 2E and Supplementary Fig. S3B). In line with these results, doxorubicin administration resulted in augmented frequency of IFN-γ–producing $CD8^+$ T lymphocytes (Fig. 2F). However, no change in the proportion of IFN-γ–producing $CD4^+$ T cells was observed (Fig. 2F). It is noteworthy that doxorubicin did not change immunosuppressive Treg frequency (Supplementary Fig. S3C). Together these results indicate that doxorubicin-mediated MDSC depletion was associated with augmented effector immune cell proliferation and function.

Importantly, we further determined that doxorubicin was significantly more potent at depleting MDSC than other chemotherapeutic agents such as cyclophosphamide, fludarabine, melphalan (Supplementary Fig. S4A), vincristine, or etoposide (Supplementary Fig. S4B), which exhibited limited effects on these cells. Of note, these drugs promoted a decrease in tumor volume similar to that induced by doxorubicin. Doxorubicin was also unique at substantially increasing the effector lymphocytes (or NK) to suppressor MDSC ratios, indicating that it is endowed with a higher degree of selectivity compared with these other drugs (Supplementary Fig. S4A and S4B). Furthermore, even in combination with cyclophosphamide, doxorubicin significantly triggered MDSC elimination and increased T lymphocyte frequency (Supplementary Fig. S4C).

The observations that doxorubicin reduces MDSC frequency and absolute number and increases effector lymphocyte proportion, resulting in an increased effector T cells to suppressor MDSC ratios, were further confirmed in the EL4 (thymoma) and EMT6 (breast cancer) mouse models (Supplementary Fig. S5A and S5B). In addition, residual MDSC isolated from EL4 or EMT6 tumor-bearing mice treated with doxorubicin exhibited reduced suppressive function (data not shown).

Doxorubicin preferentially triggers MDSC apoptotic program

We next investigated the mechanisms underlying doxorubicin-mediated elimination of MDSC and specifically explored whether this drug may trigger the MDSC apoptotic program. Flow cytometry analysis after staining of spleen cells with anti-Gr-1, anti-CD11b antibodies, Annexin V and PI, and gating on the $Gr\text{-}1^+CD11b^+$ population indicated

Published OnlineFirst November 6, 2013; DOI: 10.1158/0008-5472.CAN-13-1545

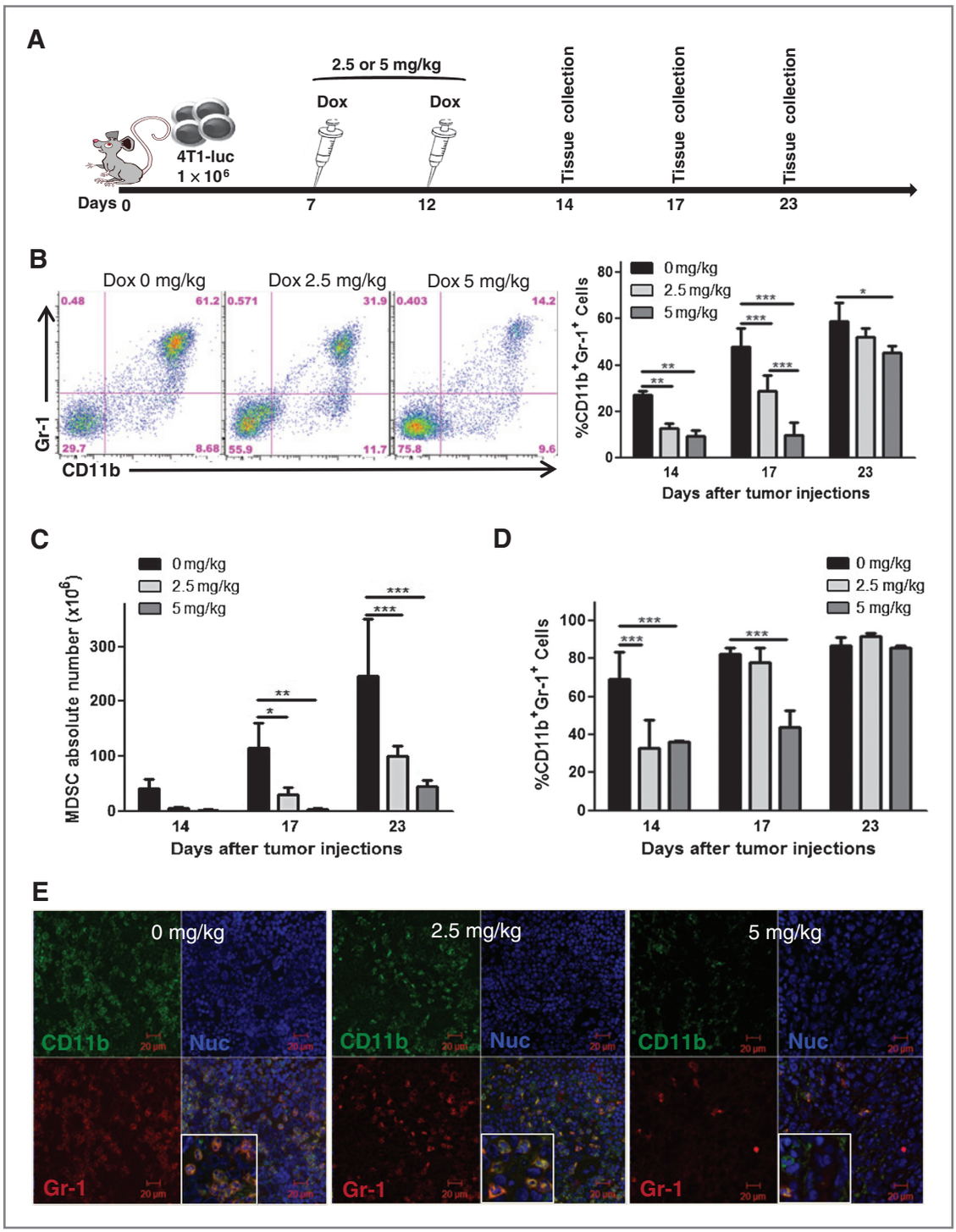

Figure 1. Doxorubicin eliminates tumor-induced MDSC. A, schematic of the experimental design followed to evaluate the effects of doxorubicin on MDSC in the 4T1 breast cancer model. Mice were injected orthotopically (mammary fat pad) with 4T1 tumor cells (1×10^6). Doxorubicin (2.5 or 5 mg/kg) was administered intravenously on day 7 and 12 posttumor injection. Spleen and blood samples were harvested and evaluated on days 14, 17, and 23. B, proportion of MDSC ($CD11b^+Gr\text{-}1^+$) in the spleen of 4T1 tumor-bearing mice post-doxorubicin treatment (right) and representative flow cytometry analysis 17 days posttumor injection (left). C, absolute number of MDSC in tumor-bearing mice treated or not with doxorubicin. D, proportion of MDSC in the blood of tumor-bearing mice after doxorubicin treatment. E, confocal microscopy analysis of $CD11b^+Gr\text{-}1^+$ cells in the spleens from untreated or doxorubicin-treated mice 17 days posttumor injection (5 days after the last doxorubicin treatment). CD11b (green), Gr-1 (red), and sytox orange nuclear staining (Nuc, blue). Scale bar, 20 μm. *, $P \leq 0.05$; **, $P \leq 0.01$; ***, $P \leq 0.001$. $n = 4$ mice per group. Data represent one of 3 experiments performed and analyzed independently.

Published OnlineFirst November 6, 2013; DOI: 10.1158/0008-5472.CAN-13-1545

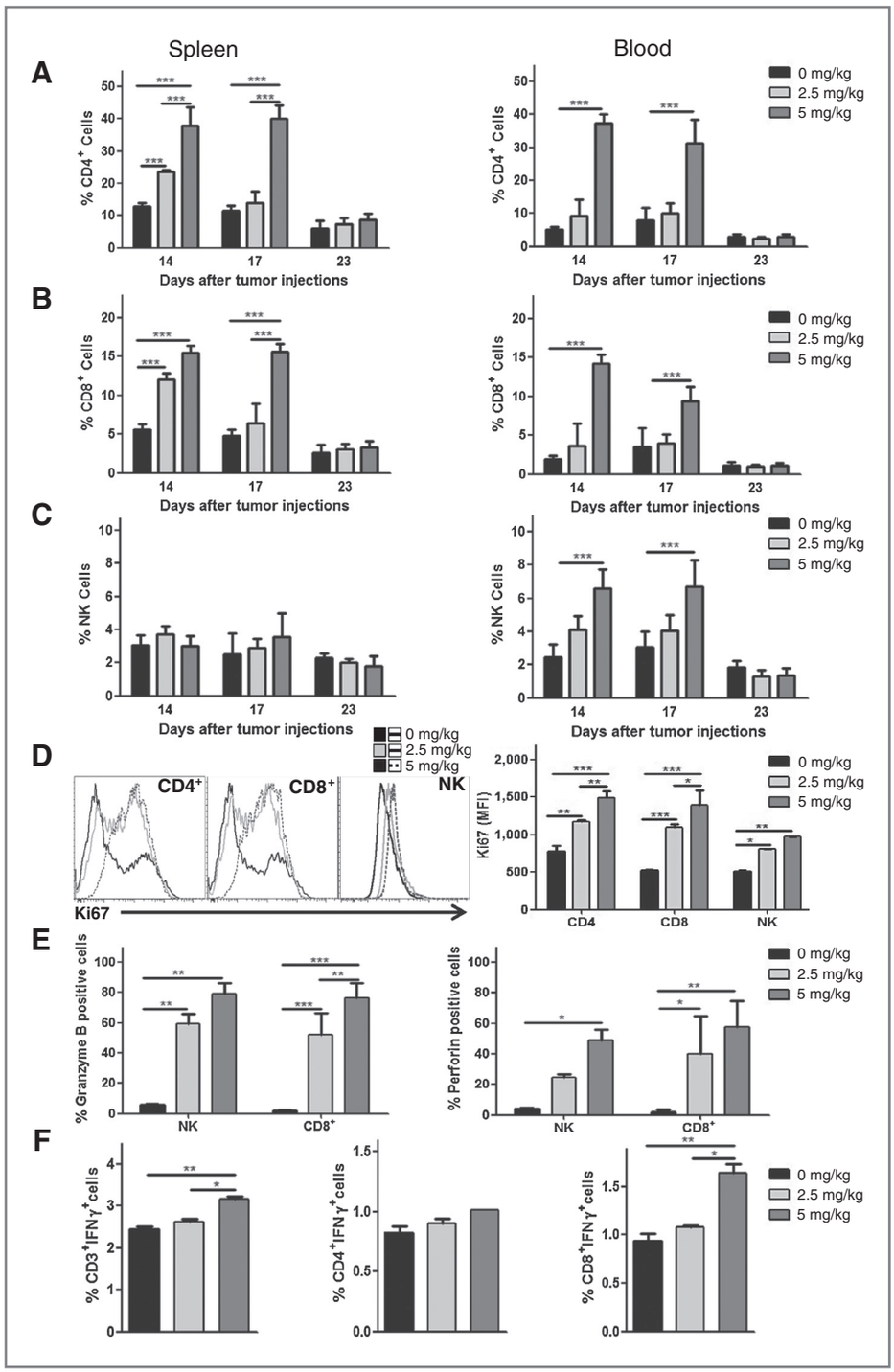

Figure 2. Doxorubicin increases the frequency, proliferation, and cytotoxic activity of effector T lymphocytes and NK. A similar experimental design as described in Fig. 1 was followed. A, frequency of $CD4^+$ T cells in the spleen (left) and blood (right) of tumor-bearing mice after doxorubicin treatment. B, proportion of $CD8^+$ T cells in the spleen (left) and blood (right) of tumor-bearing mice after doxorubicin treatment. C, NK cell frequency in the spleen (left) and blood (right) of doxorubicin-treated mice. D, analysis of Ki67 expression after gating on $CD4^+$, $CD8^+$ T lymphocytes, or NK ($DX5^+$) cells as indicated (left) and related mean fluorescent intensity (MFI; right; day 17). E, percent of $CD8^+$ T and NK cells expressing granzyme B or perforin in the spleen of doxorubicin-treated mice 17 days posttumor cell injection. F, percent of $CD3^+$, $CD4^+$, and $CD8^+$ T lymphocytes expressing IFN-γ in the spleen of tumor-bearing mice treated or not with doxorubicin (day 17). *, $P \leq 0.05$; **, $P \leq 0.01$; ***, $P \leq 0.001$. $n = 4$ mice per group. Data represent one of 3 experiments performed and analyzed independently.

that doxorubicin increased the proportion of apoptotic (Annexin V^+, PI^-) and secondary necrotic (Annexin V^+, PI^+) MDSC (Fig. 3A). Consistent with these data, caspase-3 cleavage was detected in MDSC isolated from 4T1 tumor-bearing doxorubicin-treated animals (Fig. 3B). Importantly, in line with the results depicted in Fig. 2A and B, the number of dead (apoptotic and necrotic) T lymphocytes ($CD4^+$ or $CD8^+$) was not significantly modified by doxorubicin (Fig. 3C). These data thus demonstrate that doxorubicin preferentially induced apoptosis of MDSC with no detectable toxic effect on effector T lymphocytes.

MDSC isolated from untreated tumor-bearing mice were more sensitive to doxorubicin *in vitro* than the MDSC-depleted cell population or than 4T1 cells (Fig. 3D and data not

Published OnlineFirst November 6, 2013; DOI: 10.1158/0008-5472.CAN-13-1545

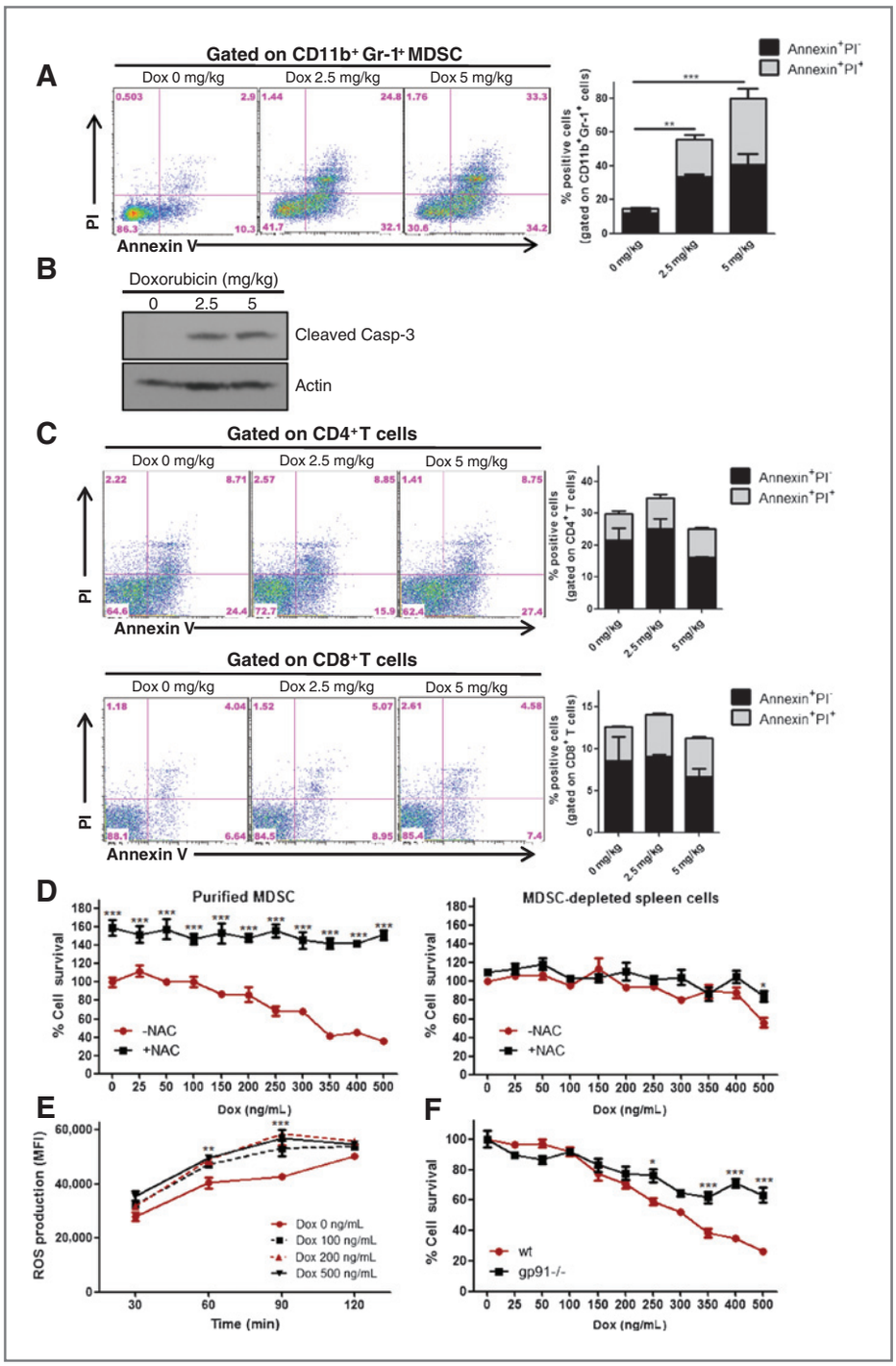

Figure 3. Doxorubicin selectively induces MDSC apoptosis. A similar experimental design as described in Fig. 1 was followed. Spleens were collected 5 days after the last doxorubicin administration. A, spleen samples were labeled for MDSC ($CD11b^+Gr\text{-}1^+$) and Annexin V and PI. Representative flow cytometry analysis (left, gated on $C11b^+Gr1^+$ cells), and proportion of apoptotic and secondary necrotic MDSC (right). B, detection of caspase-3 cleavage in MDSC isolated from mice treated or not with doxorubicin 17 days posttumor injection. C, spleen samples were labeled with anti-CD4 or anti-CD8 and Annexin V and PI. Gated $CD4^+$ or $CD8^+$ T lymphocytes were then analyzed for their Annexin V and PI status. Percent of apoptotic or secondary necrotic $CD4^+$ (top) and $CD8^+$ (bottom) T lymphocytes in doxorubicin-treated or untreated mice. Similar experimental design as in A. D, effects of doxorubicin used at the indicated concentrations on MDSC isolated from 4T1 tumor-bearing mouse spleens (or on the MDSC-depleted cell population) determined by MTT assays. Cells were cultured in quadruplicate for 30 hours with or without NAC (5 mmol/L). % cell survival = (OD_{560}[treated cells at the indicated doxorubicin concentration]/OD_{560}[untreated cells] $\times$ 100). E, analysis of ROS production by MDSC isolated from tumor-bearing mice and treated *in vitro* with the indicated concentrations of doxorubicin and for the indicated period of time. Cells were incubated with DCFDA and analyzed by flow cytometry. The mean fluorescent intensity representing ROS levels in MDSC is shown. F, same as in D, but with MDSC isolated from EL4 tumor-bearing wild type or $gp91^{-/-}$ mice. *, $P \leq 0.05$; **, $P \leq 0.01$; ***, $P \leq 0.001$. $n = 4$ mice per group. Data represent one of 3 experiments performed and analyzed independently.

shown). Treatment of these purified MDSC with *N*-acetylcysteine (NAC, an ROS scavenger) prevented their killing by doxorubicin, suggesting that ROS may play a role in this process (Fig. 3D). Consistent with this result, the levels of ROS were increased in the immediate hours following doxorubicin treatment of MDSC *in vitro* (Fig. 3E), and MDSC isolated from EL4 tumor-bearing $gp91^{-/-}$ mice (lacking the gp91phox glycosylated subunit of the NADPH oxidase flavocytochrome b558, responsible for the production of superoxide ion $O2\cdot^-$) were less sensitive to doxorubicin-mediated cytotoxicity *in vitro* (Fig. 3F). Interestingly, *in vivo*, the effects of doxorubicin administration on MDSC were partially impaired in EL4 tumor-bearing $gp91^{-/-}$ mice compared with wild-type mice (data not shown).

Published OnlineFirst November 6, 2013; DOI: 10.1158/0008-5472.CAN-13-1545

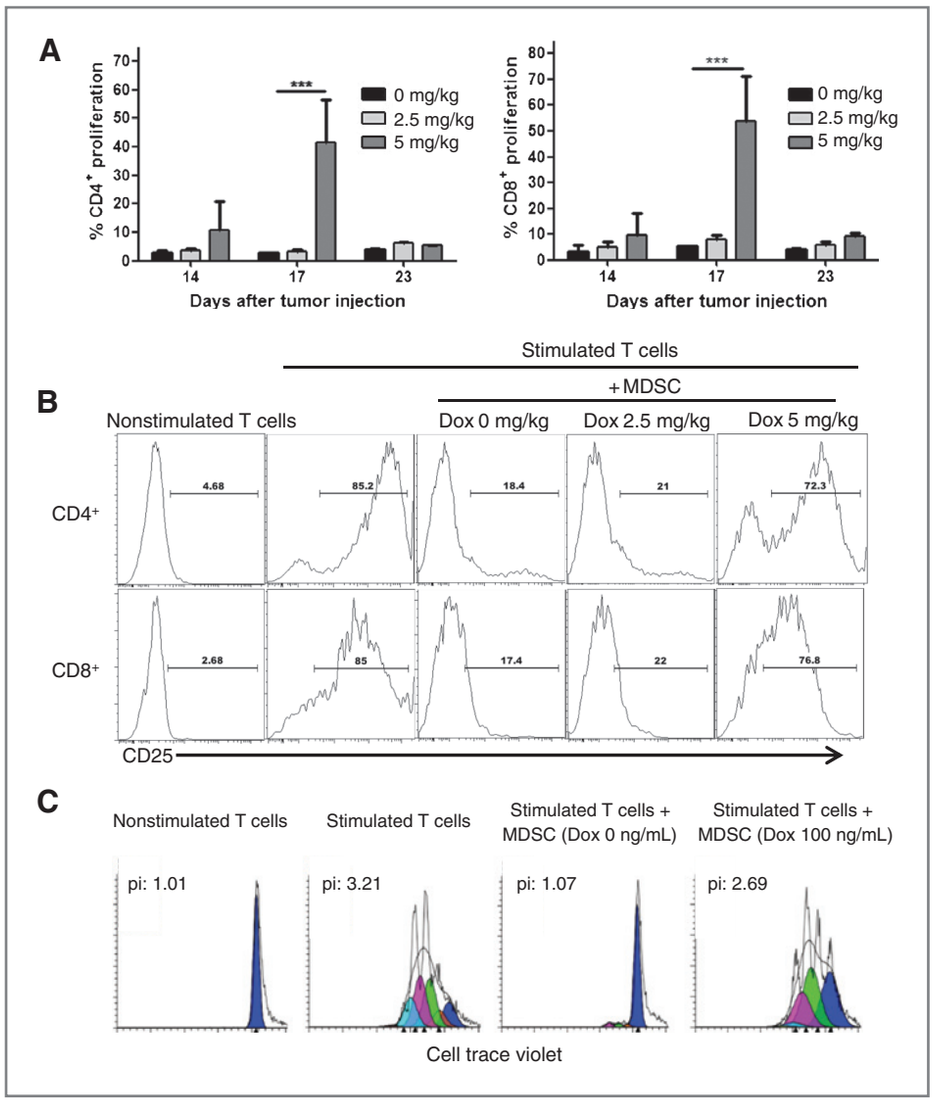

Figure 4. Doxorubicin impairs MDSC immunosuppressive function. A and B, MDSC isolated from untreated or doxorubicin-treated mice were incubated for 4 days with cell trace violet-labeled naive T cells (MDSC: T-cell ratio = 1:2). A, effects of MDSC from the indicated groups of mice on the proliferation of $CD4^+$ (left) or $CD8^+$ (right) T lymphocytes assessed by flow cytometry. B, effects of MDSC on CD25 expression by gated $CD4^+$ (top) or $CD8^+$ (bottom) T lymphocytes. C, MDSC isolated from tumor-bearing mice were treated or not *in vitro* with doxorubicin (100 ng/mL, 24 hours) and their ability to impair the proliferation of cell trace violet-labeled naive $CD4^+$ T cells induced by anti-CD3 and anti-CD28–coated activation beads was evaluated by flow cytometry. *, $P \leq 0.05$; **, $P \leq 0.01$; ***, $P \leq 0.001$. $n = 4$ mice per group. Data represent one of 2 experiments performed and analyzed independently. pi, proliferation index.

Doxorubicin impedes the suppressive activity of residual MDSC isolated from tumor-bearing mice

A cardinal characteristic of MDSC is their ability to suppress the activation and proliferation of T cells. MDSC depletion by doxorubicin was not complete as ~15% of residual MDSC could still be detected 17 days after doxorubicin administration. Therefore, it was important to determine whether the suppressive function of these remaining MDSC was affected by doxorubicin. As expected and previously reported (32), MDSC isolated from untreated tumor-bearing mice significantly inhibited T lymphocyte ($CD4^+$ and $CD8^+$) proliferation (Fig. 4A and Supplementary Fig. S6) and activation (Fig. 4B). The suppressive function of residual MDSC isolated from doxorubicin-treated tumor-bearing animals was significantly impaired (Fig. 4A and B and Supplementary Fig. S6). Exposure of MDSC isolated from untreated 4T1 tumor-bearing mice to noncytotoxic concentration of doxorubicin *in vitro* impaired their immunosuppressive function (Fig. 4C).

Various mechanisms have been implicated in MSDC suppressive function including the production of ROS or the expression of arginase-1 or IDO involved in the catabolism of arginine or tryptophan, respectively (1). Depletion of these amino acids from the microenvironment results in the inhibition of T-cell proliferation, notably through the downregulation of the ζ-chain of the TCR complex (1, 11). Similarly, ROS exhibit suppressive effects on T lymphocytes (1, 33). Five days after doxorubicin treatment of 4T1 tumor-bearing mice, the production of ROS (Fig. 5A) and the expression of arginase-1 (Fig. 5B) and IDO (Fig. 5C) by residual MDSC was impaired. Additional molecules reported for their role in MDSC development and/or immunosuppressive function such as CD73, CD39, S100A8/9, or STAT-3 were not significantly altered by doxorubicin treatment (Supplementary Fig. S7A and S7B).

Published OnlineFirst November 6, 2013; DOI: 10.1158/0008-5472.CAN-13-1545

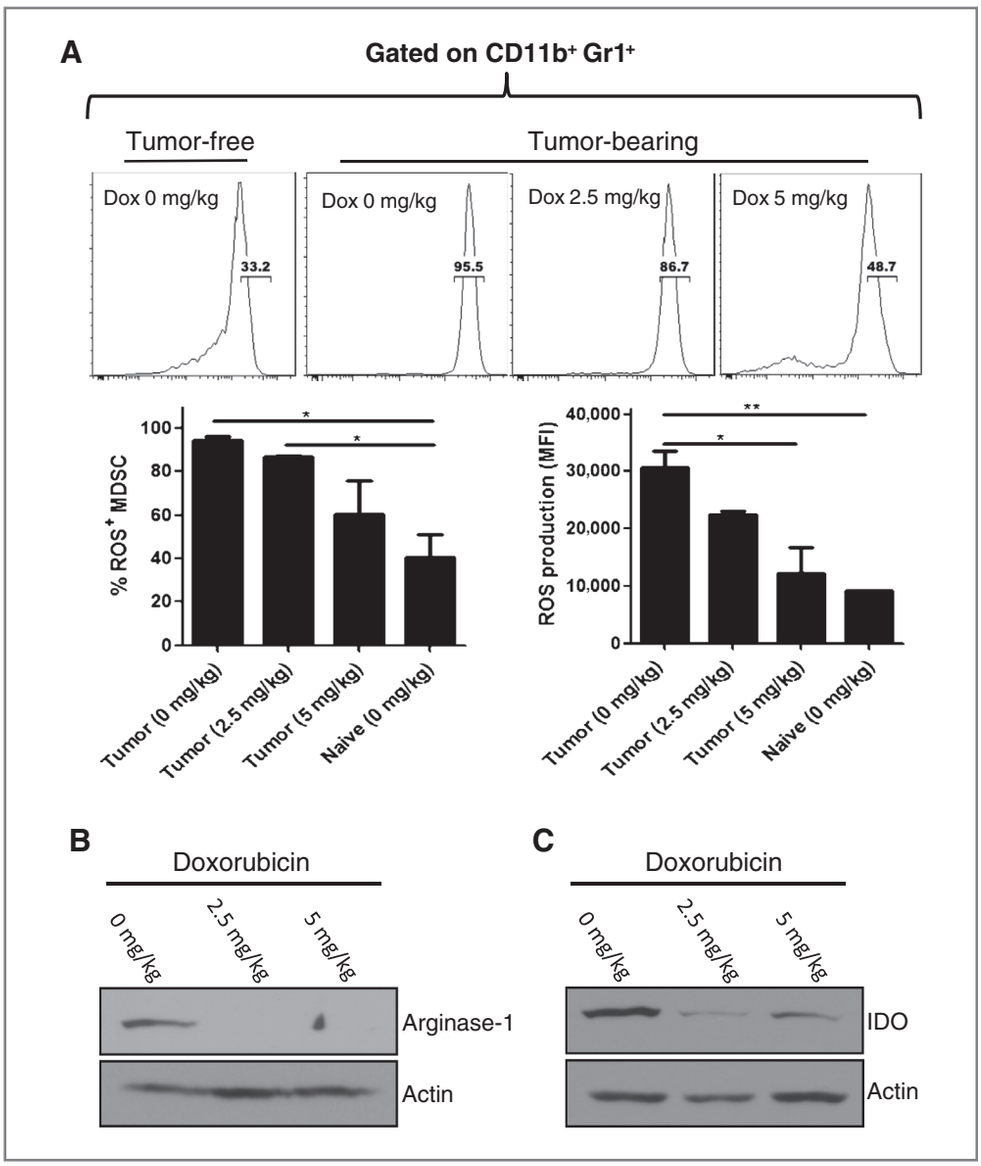

Figure 5. Doxorubicin decreases ROS production and arginase-1 and IDO expression by MDSC. A similar experimental design as described in Fig. 1 was followed. Spleens were harvested 5 days after the last doxorubicin treatment (day 17). A, analysis of ROS production by MDSC in tumor-free (tumor-free) or in tumor-bearing (tumor-bearing) mice treated with the indicated concentration of doxorubicin. Cells were incubated with DCFDA. Representative flow cytometry analysis of gated $CD11b^{+}Gr\text{-}1^{+}$ cells positive for DCFDA (top). Percent of MDSC positive for DCFDA (left bottom). Mean fluorescent intensity representing ROS level in MDSC from the indicated groups (right bottom). B and C, Western blot analysis depicting expression of arginase-1 (B) or IDO (C) in MDSC isolated from doxorubicin-treated or -untreated mice. *, $P \leq 0.05$; **, $P \leq 0.01$; ***, $P \leq 0.001$. $n = 4$ mice per group. Data represent 1 of 3 experiments performed and analyzed independently.

Previous reports have indicated that some chemotherapeutic drugs such as docetaxel can promote MDSC differentiation into macrophages (M1; ref. 20). To evaluate this possibility, MDSC from doxorubicin-treated mice were analyzed for the expression of markers expressed by M1 (CCR7) or M2 (CD206; Mannose Receptor) macrophages. The expression of these 2 cell surface markers was not detected on MDSC following doxorubicin treatment, indicating that this drug did not promote MDSC differentiation into macrophages (Supplementary Fig. S7C). Finally, further investigation indicated that the proliferation status (Ki67 expression) of residual 4T1 tumor-induced MDSC was reduced by doxorubicin therapy (not shown).

Altogether, these results indicate that 5 days after doxorubicin administration, MDSC that have not been eliminated by the drug exhibited reduced expression of arginase-1 and IDO, decreased ROS level, and curtailed immunosuppressive activity.

Published OnlineFirst November 6, 2013; DOI: 10.1158/0008-5472.CAN-13-1545

Doxorubicin acts synergistically with Th_1 or Th_{17} cell therapy

Doxorubicin depleted tumor-induced MDSC and curtailed the suppressive function of residual MDSC, thereby averting one major mechanism of cancer-mediated immunosuppression. Moreover, the proliferation status and activation of responder effector lymphocytes and NK were restored in doxorubicin-treated mice. We therefore reasoned that this drug may create a favorable environment that may allow for successful combinatory immunotherapy. To address this hypothesis, we evaluated a chemo-immunotherapy regimen consisting of doxorubicin followed by infusion of T helper lymphocytes.

Th_{17} lymphocytes represent a recently described subset of T helper cells with controversial effects on tumor development. Recent reports have demonstrated that Th_{17} generated *in vitro* have the potential to promote the development of $CD8^+$ T lymphocyte-dependent immune response and to impair tumor growth (34). Th_1 can also promote antitumor immunity (35). In our current study, mice bearing established 4T1 tumors were treated with doxorubicin and received either Th_1 or Th_{17} lymphocytes generated *in vitro* from naive $CD4^+$ T cells (Supplementary Fig. S8A and S8B) as depicted in Fig. 6A. The chemoimmunotherapeutic regimen significantly reduced the number of 4T1 metastatic nodules in the lungs and impaired tumor growth when compared with the monotherapies (Fig. 6B and Supplementary Fig. S8C). Importantly, MDSC depletion persisted in mice treated with doxorubicin plus Th_1 or Th_{17} cells, whereas these cells eventually re-expanded post-treatment in mice receiving doxorubicin alone (Fig. 6C and D). Consistent with these results, the frequency of $CD8^+$ and $CD4^+$ T lymphocytes was significantly increased in doxorubicin plus Th_1- or Th_{17}-treated animals (Fig. 6D), but NK proportion remained unchanged (data not shown). These data thus indicate that doxorubicin administration resulted in the promotion of a favorable environment fostering the antitumoral efficacy of Th_1 and Th_{17} lymphocytes.

Doxorubicin induces apoptosis of MDSC isolated from patients with cancer

To determine whether similar effects of doxorubicin can be observed on human MDSC, $CD33^+$ cells were isolated from the blood of patients with different types of cancer ($n = 10$). $CD33^+$ cells exhibited a phenotype consistent with that reported for human MDSC (Fig. 7A; ref. 36) and importantly were endowed with significant suppressive capabilities (Fig. 7B). Our results indicate that these immunosuppressive cells were sensitive to doxorubicin-induced cell death (Fig. 7C and E). Importantly, $CD33^-$ depleted cells ($CD33^-$) from the same patients were significantly less sensitive to doxorubicin (Fig. 7D and E), indicating that this chemotherapeutic molecule preferentially targets MDSC. $CD3^+$ T cells were also minimally affected by doxorubicin (not shown). These results thus suggest that doxorubicin exhibit effects on human MDSC comparable to those observed on mouse MDSC, thus supporting the implementation of this drug in clinical chemoimmunotherapeutic approaches.

Discussion

The development of malignant tumors is commonly associated with the occurrence and persistence of an immunosuppressive environment. The expansion of MDSC, a main suppressive cell population (13), has been widely documented in many animal tumor models as well as in patients with different types of cancers and represents a major obstacle for efficient cancer immunotherapy (5, 9, 10). Several strategies have been explored to either eliminate or curtail, the immunosuppressive function of MDSC. Depletion of $Gr\text{-}1^+$ MDSC using anti-Gr-1 monoclonal antibody resulted in restored T-cell antitumor activity. However, anti-Gr-1 also led to the elimination of mature granulocytes and was associated with severe immunosuppression (13). The promotion of MDSC differentiation using ATRA, a natural metabolite of vitamin A, has also been considered. ATRA administration enhanced T lymphocyte function and fostered the efficacy of cancer vaccines (14). In recent years, evidence has been provided that chemotherapeutic drugs can not only kill tumor cells, but also enhance antitumor immunity through different mechanisms (37). Chemotherapeutic agents can promote the function of antigen presenting cells, NK, and T lymphocytes (23, 26, 37) but may also negatively target immunosuppressive cells such as Treg or MDSC (17, 19, 20, 38, 39). For instance, gemcitabine has been reported to deplete MDSC in tumor-bearing mice, resulting in enhanced antitumor immunity (17–20). Additional reports have demonstrated that 5-Fluorouracil (19), or docetaxel (20), can eliminate, impede the suppressive function, or promote the differentiation of MDSC.

Doxorubicin has been a key chemotherapeutic agent used against a variety of human cancers. More recently, this drug has been widely studied for its ability to modulate anticancer immunity (23–26, 28). Reports have demonstrated that doxorubicin induces an "immunogenic type" of tumor cell death and promotes antitumor immune responses (23). In this study, we highlight a novel property of doxorubicin: its ability to avert a major mechanism of tumor-induced immunosuppression by eliminating and inactivating tumor-induced MDSC. We established that doxorubicin administration reduced the number of MDSC in the spleen, blood, and in the tumor beds of animals bearing established 4T1 mammary tumors. Importantly, doxorubicin selectively eliminated MDSC while enhancing the proliferation status, activation, cytokine production of effector T lymphocytes and/or NK cells. This primary targeting of MDSC while effector T cells (and NK) were spared translated into a substantial increase in effector lymphocytes to MDSC ratios. Compared with the other chemotherapeutic drugs that we evaluated, doxorubicin was endowed with the highest degree of selectivity. Indeed, although associated with a reduction of tumor volume comparable to that observed after doxorubicin treatment, most of these other agents had limited effects on MDSC and some of them, such as cyclophosphamide, even led to a slight increase in MDSC as they targeted T cells.

Published OnlineFirst November 6, 2013; DOI: 10.1158/0008-5472.CAN-13-1545

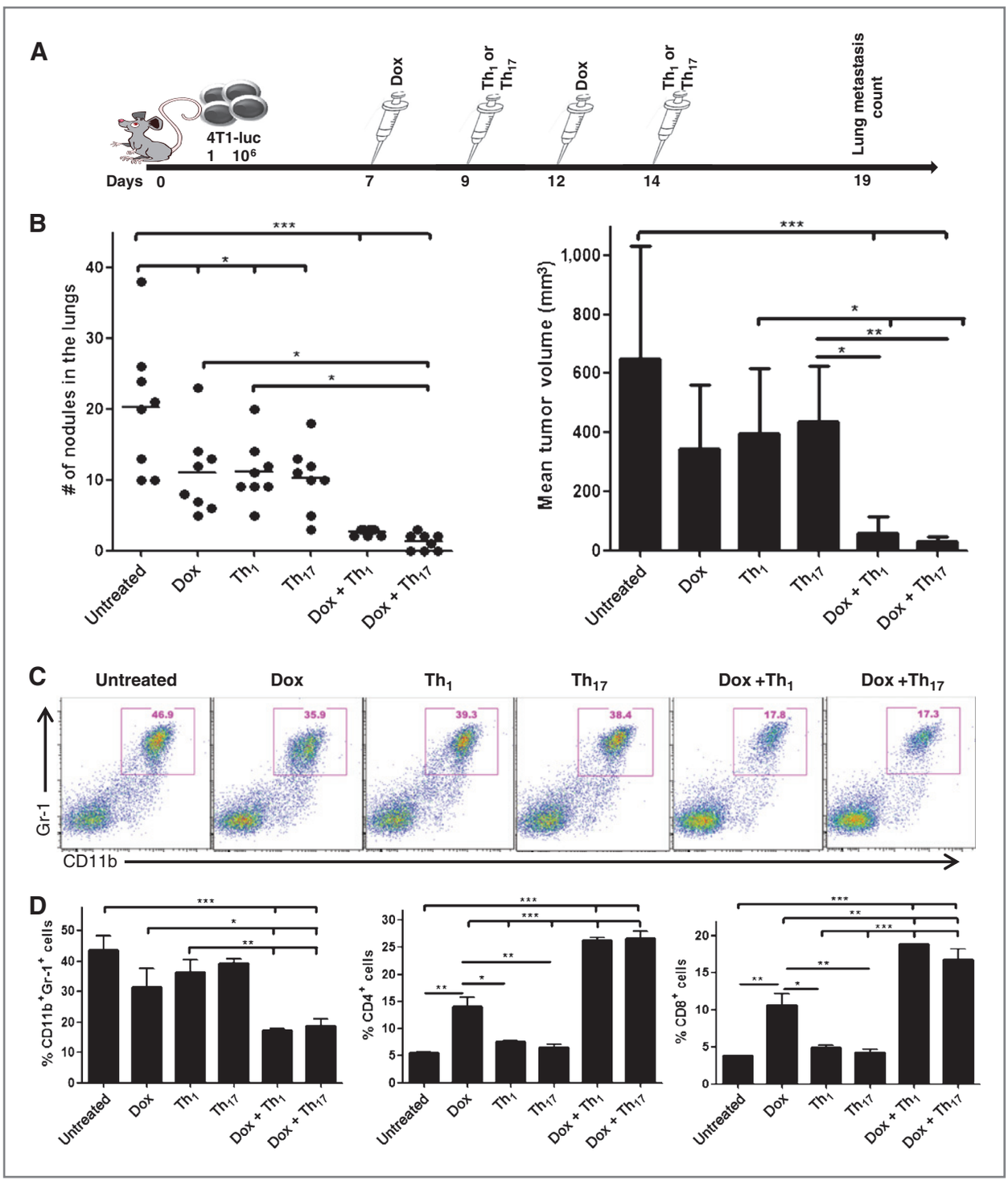

Figure 6. The combination of doxorubicin and Th_1 or Th_{17} impairs 4T1 tumor development. Mice were injected orthotopically (mammary fat pad) with 4T1 tumor cells (1×10^6). Doxorubicin (5 mg/kg) was injected intravenously on day 7 and 12 posttumor cell injection. Th_1 or Th_{17} lymphocytes were administered on day 9 and 14 posttumor cell injection, intravenously (1×10^6) and intratumoraly (2×10^6). Tumor volume and number of metastatic nodules were evaluated on day 19 posttumor injection. A, schematic of the experimental design. B, number of metastatic nodules (left) and tumor volume (right). C, representative flow cytometry analysis of MDSC frequency in mice administered with the indicated therapies. D, proportion of MDSC, $CD4^+$, and $CD8^+$ T cells in mice receiving the indicated therapies; $n = 8$ mice per group. Data are representative of 3 independent experiments. *, $P \leq 0.05$; **, $P \leq 0.01$; ***, $P \leq 0.001$.

Published OnlineFirst November 6, 2013; DOI: 10.1158/0008-5472.CAN-13-1545

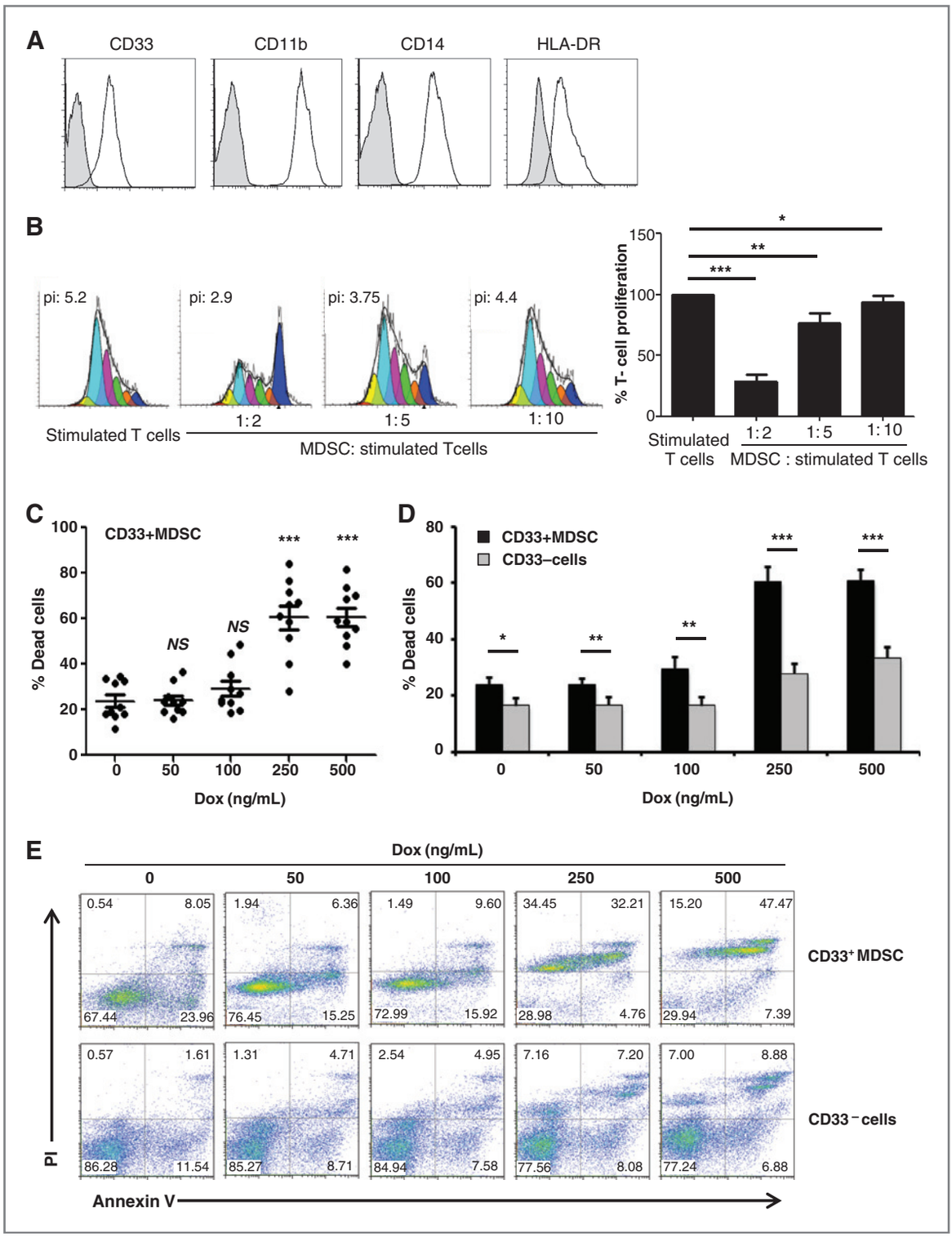

Figure 7. Doxorubicin selectively kills MDSC isolated from patients with cancer. $CD33^+$ cells were isolated from cancer patient PBMCs by magnetic cell sorting. A, phenotypic analysis of the isolated cells. Representative results of $n = 10$ patients. B, ability of the $CD33^+$ purified cells to impair the proliferation of cell trace violet-labeled T lymphocytes induced with anti-CD3 and anti-CD28–conjugated microbeads (at the indicated MDSC to T-cell ratios). pi, proliferation index. C and D, purified $CD33^+$ MDSC or $CD33^-$ cells were exposed to the indicated concentrations of doxorubicin for 24 hours and stained with Annexin V and PI (% dead cells = % of PI^+ +% $AnnexinV^+PI^-$ cells). A total of $n = 10$ patients were analyzed. E, representative dot plots obtained with $CD33^+$ MDSC or $CD33^-$ cells isolated from a patient with cancer. (*, $P \leq 0.05$; **, $P \leq 0.01$; ***, $P \leq 0.001$).

Published OnlineFirst November 6, 2013; DOI: 10.1158/0008-5472.CAN-13-1545

Of therapeutic relevance, the addition of doxorubicin to cyclophosphamide resulted in a significant elimination of MDSC similar to that observed when doxorubicin was administered alone. This peculiar property of doxorubicin further highlights the interest and advantage of using this drug as a potent immunomodulatory agent in chemoimmunotherapeutic approaches.

Further investigation indicated that doxorubicin selectively triggered the apoptotic program of MDSC. No change in the apoptosis rate of T or NK cells was detected post-doxorubicin treatment compared with untreated groups. This selective effect may be partly explained by the preferential targeting of highly proliferative cells by doxorubicin. Indeed, MDSC in untreated tumor-bearing mice expressed high level of Ki67, a marker of cell proliferation (data not shown), whereas T lymphocyte proliferation was low in untreated tumor-bearing mice. The triggering of apoptosis by doxorubicin through the induction of ROS production has been described in tumor and normal cells such as cardiomyocytes (40). *In vitro*, the ROS scavenger NAC impaired doxorubicin-mediated elimination of MDSC, and MDSC isolated from gp91$^{-/-}$ mice were less sensitive to doxorubicin. The effects of doxorubicin on MDSC were partially impaired in EL4 tumor-bearing gp91$^{-/-}$ mice. These results strongly suggest that, early after its administration, doxorubicin may induce ROS-dependent triggering of the MDSC apoptotic program, resulting in the rapid elimination of most of these cells. Of note, MDSC that were not eliminated and that were found later (5 days) after doxorubicin treatment exhibited an overall impaired suppressive activity, which, at this time was associated with a reduction of ROS production.

A previous report has indicated that docetaxel reduced MDSC number by promoting their differentiation into M1 macrophages (20). We did not detect any changes in the expression of M1 or M2 macrophage markers on MDSC following doxorubicin treatment. In addition, no change in the frequency of macrophages or DC was detected in the treated mice. However, as mentioned earlier, the suppressive function of the limited number of residual MDSC that were not depleted by doxorubicin was significantly impaired.

Because doxorubicin administration induced MDSC depletion and was associated with restored T lymphocyte activity, we reasoned that it may create a favorable environment for efficient immunotherapy. Infusion of *in vitro* generated Th_1 cells has been reported to promote antitumor immunity (35). Th_{17} lymphocytes have recently emerged as a new effector $CD4^+$ T helper cell subset (41) exhibiting effector functions distinct from Th_1 and Th2 lymphocytes (42). Th_{17} have been identified as major contributors to the pathogenesis of multiple autoimmune conditions in animals and humans (42). However, the role of Th_{17} cells in cancer remains controversial. Although some studies have documented the antitumoral efficacy of these cells (34, 43–45), others have reported on their immunosuppressive properties (46). These conflicting results related to the protumoral versus antitumoral properties of Th_{17} may be explained by the high degree of plasticity of these cells (47–49). Supporting the antitumoral role of *in vitro* polarized Th_{17}, Muranski and colleagues demonstrated that adoptive Th_{17} cell therapy has the potential to eliminate established tumors. The antitumoral efficacy of Th_{17} lymphocytes depended on their ability to produce both IFN-γ and IL-17 (43, 44). Consistent with these studies, our own results indicated that Th_{17} generated from OT-II mice exhibit antitumoral effects against B16-OVA melanoma (unpublished data). In this study, we demonstrated that the therapeutic efficacy of adoptively transferred Th_1 or Th_{17} lymphocytes was significantly enhanced by doxorubicin administration, resulting in impaired development of the highly metastatic 4T1 mammary carcinoma.

Doxorubicin is widely used in chemotherapeutic regimen primarily for its conventional direct tumoricidal activity. Here we highlight a new application for this drug as a selective MDSC-targeting agent, which can be used to overcome a major mechanism of tumor immune evasion. These results advocate for the implementation of doxorubicin in combination strategies to enhance the efficacy of immunotherapy.

Disclosure of Potential Conflicts of Interest

No potential conflicts of interest were disclosed.

Authors' Contributions

Conception and design: D. Alizadeh, N. Larmonier
Development of methodology: D. Alizadeh, M. Trad, B. Bonnotte, N. Larmonier
Acquisition of data (provided animals, acquired and managed patients, provided facilities, etc.): D. Alizadeh, M. Trad, N.T. Hanke, C.B. Larmonier, B. Bonnotte
Analysis and interpretation of data (e.g., statistical analysis, biostatistics, computational analysis): D. Alizadeh, M. Trad, C.B. Larmonier, N. Janikashvili, B. Bonnotte, E. Katsanis, N. Larmonier
Writing, review, and/or revision of the manuscript: D. Alizadeh, M. Trad, N. Janikashvili, B. Bonnotte, E. Katsanis, N. Larmonier
Administrative, technical, or material support (i.e., reporting or organizing data, constructing databases): D. Alizadeh
Study supervision: D. Alizadeh, N. Larmonier

Acknowledgments

The authors thank Dr. C.J. LaCasse, J. Stokes, E.M. Assimacopoulos (University of Arizona, Department of Pediatrics), and P. Campbell (AZCC/ARL-Division of Biotechnology Cytometry Core Facility, Arizona Cancer Center, University of Arizona, Tucson, AZ) for technical assistance.

Grant Support

This work was funded in part by the National Institutes of Health grant R01CA104926 (N. Larmonier and E. Katsanis), Cancer Biology Training Grant T32CA009213 (D. Alizadeh), AZ Cancer Center Grant CA023074, Cancer Center Support Grant CA023074, PANDA Funds (N. Larmonier and E. Katsanis), and a grant from La Ligue contre le Cancer (Coordination interrégionale du Grand-Est; B Bonnette).

The costs of publication of this article were defrayed in part by the payment of page charges. This article must therefore be hereby marked *advertisement* in accordance with 18 U.S.C. Section 1734 solely to indicate this fact.

Received May 30, 2013; revised September 27, 2013; accepted October 12, 2013; published OnlineFirst November 6, 2013.

References

1. Gabrilovich DI, Nagaraj S. Myeloid-derived suppressor cells as regulators of the immune system. Nat Rev Immunol 2009;9:162–74.
2. Ostrand-Rosenberg S, Sinha P. Myeloid-derived suppressor cells: linking inflammation and cancer. J Immunol 2009;182:4499–506.

Published OnlineFirst November 6, 2013; DOI: 10.1158/0008-5472.CAN-13-1545

3. Serafini P, De Santo C, Marigo I, Cingarlini S, Dolcetti L, Gallina G, et al. Derangement of immune responses by myeloid suppressor cells. Cancer Immunol Immunother 2004;53:64–72.
4. Bunt SK, Sinha P, Clements VK, Leips J, Ostrand-Rosenberg S. Inflammation induces myeloid-derived suppressor cells that facilitate tumor progression. J Immunol 2006;176:284–90.
5. Youn JI, Nagaraj S, Collazo M, Gabrilovich DI. Subsets of myeloid-derived suppressor cells in tumor-bearing mice. J Immunol 2008;181:5791–802.
6. Peranzoni E, Zilio S, Marigo I, Dolcetti L, Zanovello P, Mandruzzato S, et al. Myeloid-derived suppressor cell heterogeneity and subset definition. Curr Opin Immunol 2010;22:238–44.
7. Ochoa AC, Zea AH, Hernandez C, Rodriguez PC. Arginase, prostaglandins, and myeloid-derived suppressor cells in renal cell carcinoma. Clin Cancer Res 2007;13:721s–6s.
8. Beck BH, Kim HG, Kim H, Samuel S, Liu Z, Shrestha R, et al. Adoptively transferred *ex vivo* expanded gammadelta-T cells mediate *in vivo* antitumor activity in preclinical mouse models of breast cancer. Breast Cancer Res Treat 2010;122:135–44.
9. Younos I, Donkor M, Hoke T, Dafferner A, Samson H, Westphal S, et al. Tumor- and organ-dependent infiltration by myeloid-derived suppressor cells. Int Immunopharmacol 2011;11:816–26.
10. Almand B, Clark JI, Nikitina E, van Beynen J, English NR, Knight SC, et al. Increased production of immature myeloid cells in cancer patients: a mechanism of immunosuppression in cancer. J Immunol 2001;166:678–89.
11. Ostrand-Rosenberg S. Myeloid-derived suppressor cells: more mechanisms for inhibiting antitumor immunity. Cancer Immunol Immunother 2010;59:1593–600.
12. Gabrilovich DI, Ostrand-Rosenberg S, Bronte V. Coordinated regulation of myeloid cells by tumours. Nat Rev Immunol 2012;12:253–68.
13. Bronte V, Serafini P, Apolloni E, Zanovello P. Tumor-induced immune dysfunctions caused by myeloid suppressor cells. J Immunother 2001;24:431–46.
14. Kusmartsev S, Cheng F, Yu B, Nefedova Y, Sotomayor E, Lush R, et al. All-trans-retinoic acid eliminates immature myeloid cells from tumor-bearing mice and improves the effect of vaccination. Cancer Res 2003;63:4441–9.
15. Nefedova Y, Fishman M, Sherman S, Wang X, Beg AA, Gabrilovich DI. Mechanism of all-trans retinoic acid effect on tumor-associated myeloid-derived suppressor cells. Cancer Res 2007;67:11021–8.
16. Mirza N, Fishman M, Fricke I, Dunn M, Neuger AM, Frost TJ, et al. All-trans-retinoic acid improves differentiation of myeloid cells and immune response in cancer patients. Cancer Res 2006;66:9299–307.
17. Suzuki E, Kapoor V, Jassar AS, Kaiser LR, Albelda SM. Gemcitabine selectively eliminates splenic Gr-1+/CD11b+ myeloid suppressor cells in tumor-bearing animals and enhances antitumor immune activity. Clin Cancer Res 2005;11:6713–21.
18. Bunt SK, Mohr AM, Bailey JM, Grandgenett PM, Hollingsworth MA. Rosiglitazone and Gemcitabine in combination reduces immune suppression and modulates T cell populations in pancreatic cancer. Cancer Immunol Immunother 2013;62:225–36.
19. Vincent J, Mignot G, Chalmin F, Ladoire S, Bruchard M, Chevriaux A, et al. 5-Fluorouracil selectively kills tumor-associated myeloid-derived suppressor cells resulting in enhanced T cell-dependent antitumor immunity. Cancer Res 2010;70:3052–61.
20. Kodumudi KN, Woan K, Gilvary DL, Sahakian E, Wei S, Djeu JY. A novel chemoimmunomodulating property of docetaxel: suppression of myeloid-derived suppressor cells in tumor bearers. Clin Cancer Res 2010;16:4583–94.
21. Tacar O, Sriamornsak P, Dass CR. Doxorubicin: an update on anticancer molecular action, toxicity and novel drug delivery systems. J Pharm Pharmacol 2013;65:157–70.
22. Bandyopadhyay A, Wang L, Agyin J, Tang Y, Lin S, Yeh IT, et al. Doxorubicin in combination with a small TGF-β inhibitor: a potential novel therapy for metastatic breast cancer in mouse models. PLoS One 2010;5:e10365.
23. Casares N, Pequignot MO, Tesniere A, Ghiringhelli F, Roux S, Chaput N, et al. Caspase-dependent immunogenicity of doxorubicin-induced tumor cell death. J Exp Med 2005;202:1691–701.
24. Eralp Y, Wang X, Wang JP, Maughan MF, Polo JM, Lachman LB. Doxorubicin and paclitaxel enhance the antitumor efficacy of vaccines directed against HER 2/neu in a murine mammary carcinoma model. Breast Cancer Res 2004;6:R275–83.
25. Panis C, Lemos LG, Victorino VJ, Herrera AC, Campos FC, Colado Simao AN, et al. Immunological effects of taxol and adryamicin in breast cancer patients. Cancer Immunol Immunother 2012;61:481–8.
26. Mattarollo SR, Loi S, Duret H, Ma Y, Zitvogel L, Smyth MJ. Pivotal role of innate and adaptive immunity in anthracycline chemotherapy of established tumors. Cancer Res 2011;71:4809–20.
27. Obeid M, Tesniere A, Ghiringhelli F, Fimia GM, Apetoh L, Perfettini JL, et al. Calreticulin exposure dictates the immunogenicity of cancer cell death. Nat Med 2007;13:54–61.
28. Ramakrishnan R, Assudani D, Nagaraj S, Hunter T, Cho HI, Antonia S, et al. Chemotherapy enhances tumor cell susceptibility to CTL-mediated killing during cancer immunotherapy in mice. J Clin Invest 2010;120:1111–24.
29. Eruslanov E, Kusmartsev S. Identification of ROS using oxidized DCFDA and flow-cytometry. Methods Mol Biol 2010;594:57–72.
30. DuPre SA, Redelman D, Hunter KW Jr. The mouse mammary carcinoma 4T1: characterization of the cellular landscape of primary tumours and metastatic tumour foci. Int J Exp Pathol 2007;88:351–60.
31. Tao K, Fang M, Alroy J, Sahagian GG. Imagable 4T1 model for the study of late stage breast cancer. BMC Cancer 2008;8:228.
32. Centuori SM, Trad M, LaCasse CJ, Alizadeh D, Larmonier CB, Hanke NT, et al. Myeloid-derived suppressor cells from tumor-bearing mice impair TGF-β-induced differentiation of CD4+CD25+FoxP3+ Tregs from CD4+CD25−FoxP3− T cells. J Leukoc Biol 2012;92:987–97.
33. Corzo CA, Cotter MJ, Cheng P, Cheng F, Kusmartsev S, Sotomayor E, et al. Mechanism regulating reactive oxygen species in tumor-induced myeloid-derived suppressor cells. J Immunol 2009;182:5693–701.
34. Martin-Orozco N, Muranski P, Chung Y, Yang XO, Yamazaki T, Lu S, et al. T helper 17 cells promote cytotoxic T cell activation in tumor immunity. Immunity 2009;31:787–98.
35. Janikashvili N, LaCasse CJ, Larmonier C, Trad M, Herrell A, Bustamante S, et al. Allogeneic effector/memory Th-1 cells impair FoxP3+ regulatory T lymphocytes and synergize with chaperone-rich cell lysate vaccine to treat leukemia. Blood 2011;117:1555–64.
36. Filipazzi P, Huber V, Rivoltini L. Phenotype, function and clinical implications of myeloid-derived suppressor cells in cancer patients. Cancer Immunol Immunother 2012;61:255–63.
37. Galluzzi L, Senovilla L, Zitvogel L, Kroemer G. The secret ally: immunostimulation by anticancer drugs. Nat Rev Drug Discov 2012;11:215–33.
38. Ghiringhelli F, Larmonier N, Schmitt E, Parcellier A, Cathelin D, Garrido C, et al. CD4+CD25+ regulatory T cells suppress tumor immunity but are sensitive to cyclophosphamide which allows immunotherapy of established tumors to be curative. Eur J Immunol 2004;34:336–44.
39. Ghiringhelli F, Menard C, Puig PE, Ladoire S, Roux S, Martin F, et al. Metronomic cyclophosphamide regimen selectively depletes CD4+CD25+ regulatory T cells and restores T and NK effector functions in end stage cancer patients. Cancer Immunol Immunother 2007;56:641–8.
40. Wang S, Konorev EA, Kotamraju S, Joseph J, Kalivendi S, Kalyanaraman B. Doxorubicin induces apoptosis in normal and tumor cells via distinctly different mechanisms. intermediacy of H(2)O(2)- and p53-dependent pathways. J Biol Chem 2004;279:25535–43.
41. Bettelli E, Korn T, Kuchroo VK. Th17: the third member of the effector T cell trilogy. Curr Opin Immunol 2007;19:652–7.
42. Korn T, Bettelli E, Oukka M, Kuchroo VK. IL-17 and Th17 Cells. Annu Rev Immunol 2009;27:485–517.
43. Muranski P, Boni A, Antony PA, Cassard L, Irvine KR, Kaiser A, et al. Tumor-specific Th17-polarized cells eradicate large established melanoma. Blood 2008;112:362–73.

Published OnlineFirst November 6, 2013; DOI: 10.1158/0008-5472.CAN-13-1545

44. Muranski P, Borman ZA, Kerkar SP, Klebanoff CA, Ji Y, Sanchez-Perez L, et al. Th17 cells are long lived and retain a stem cell-like molecular signature. Immunity 2011;35: 972–85.
45. Wei S, Zhao E, Kryczek I, Zou W. Th17 cells have stem cell-like features and promote long-term immunity. Oncoimmunology 2012; 1:516–9.
46. Chalmin F, Mignot G, Bruchard M, Chevriaux A, Vegran F, Hichami A, et al. Stat3 and Gfi-1 transcription factors control Th17 cell immunosuppressive activity via the regulation of ectonucleotidase expression. Immunity 2012;36:362–73.
47. Martin F, Apetoh L, Ghiringhelli F. Controversies on the role of Th17 in cancer: a TGF-β-dependent immunosuppressive activity? Trends Mol Med 2012;18:742–9.
48. Muranski P, Restifo NP. Essentials of Th17 cell commitment and plasticity. Blood 2013;121:2402–14.
49. Zou W, Restifo NP. T(H)17 cells in tumour immunity and immunotherapy. Nat Rev Immunol 2010;10:248–56.

Supplemental Figure S1: MDSC expansion positively correlates with 4T1 tumor progression.

Six to eight week-old Balb/c mice were injected with 1×10^6 4T1 cells (mammary fat pad). MDSC ($CD11b^+Gr\text{-}1^+$) frequency was analyzed 1, 2, 3, 4 and 4.5 weeks post-tumor injection. Percentage of $CD11b^+Gr\text{-}1^+$ cells in the spleen of mice bearing 4T1 tumors (upper panels). Bioluminescent imaging of 4T1 tumor progression and lung metastases at the same time points (lower panels). n=4 mice per time point. One representative mouse out of 4 is shown. Two independent experiments were performed.

Supplemental Figure S2: Doxorubicin eliminates MDSC in the tumor beds.

Mice were injected orthotopically (mammary fat pad) with 4T1 tumor cells (1×10^6). Doxorubicin (2.5 or 5 mg/kg) was administered intravenously on day 7 and 12 post-tumor cell injection. A, MDSC absolute number in the tumor of mice treated with the indicated doses of doxorubicin. B, Proportion of MDSC in the tumor of mice treated with the indicated doses of doxorubicin. C, Confocal microscopy analysis of 4T1 tumors from mice treated with the indicated doses of doxorubicin. Tumor sections were stained for CD11b (green), Gr-1 (red) and sytox orange (nuclear staining, Nuc, blue); Scale bar: 50 μm. D, Analysis of monocytic MDSC by flow cytometry in mice treated with the indicated doses of doxorubicin after gating on CD11b+ cells. *P ≤ 0.05; **P ≤ 0.01; ***P ≤ 0.001. n=4 mice per group. Data represent one of 2 experiments performed and analyzed independently.

Supplemental Figure S3: Doxorubicin administration increases the effector to suppressor ratios in 4T1 tumor bearing mice but does not alter Treg numbers

Mice bearing 4T1 tumors were treated with doxorubicin (2.5 or 5 mg/kg) on day 7 and 12 and spleens were analyzed on day 14, 17 and 23 post-tumor cell injection. A, Ratio of CD4+ (top panels), CD8+ (middle panels) T lymphocyte, or NK cell (lower panels) to MDSC at the indicated time points in mice treated with the indicated doses of doxorubicin. B, Expression of perforin or granzyme B by CD8+ T and NK cells 17 days post-tumor injection (MFI values). C, Proportion of FoxP3+ Treg in mice treated with the indicated doses of doxorubicin 17 days post tumor cell injection (right panel) and a representative dot plot showing CD25 and FoxP3 expression after gating on CD4+ T cells (left). *$P \leq 0.05$; **$P \leq 0.01$; ***$P \leq 0.001$. n=4 mice per group. Data represent one of 2 experiments performed and analyzed independently.

Supplemental Figure S4: Doxorubicin is more efficient at selectively eliminating MDSC than cyclophosphamide, fludarabine, melphalan, vinblastine or etoposide. Mice bearing established 4T1 tumors were treated with doxorubicin (5 mg/kg; i.v.), cyclophosphamide (50 mg/kg; i.p.), fludarabine (50 mg/kg; i.p.), melphalan (5 mg/kg; i.p.), vincristine (1 mg/kg; i.v.) or etoposide (5 mg/kg; i.p.) on days 7 and 12 post tumor cell injections. Tumor volume was measured and spleens were collected and analyzed on day 17 post-tumor cell injection. All drugs reduced tumor volume to a comparable manner. A-B, Proportion and absolute number of MDSC (CD11b+Gr-1+) and proportion of T cells (CD4+, CD8+) and NK cells (top panels). Effector cells to suppressor MDSC ratios (bottom panels). C, Mice bearing 4T1 tumors were treated either with doxorubicin (5 mg/kg; i.v.) alone, cyclophosphamide (50 mg/kg; i.p.) alone, or doxorubicin (5 mg/kg; i.v.) plus cyclophosphamide (50 mg/kg; i.p.), on days 7 and 12 post tumor injections. Tumor volume and frequency of MDSC and effector cells were determined (top panels). Effector cells to suppressor MDSC ratios (bottom panels). *$P \leq 0.05$; **$P \leq 0.01$; ***$P \leq 0.001$. n=4 mice per group. Data represent one of 2 experiments performed and analyzed independently.

Supplemental Figure S5: Doxorubicin eliminates MDSC in mice bearing EMT6 breast cancer or EL4 thymoma. Mice were injected with (A) EL4 (1×106; subcutanously) or (B) EMT6 (1×106; orthotopically) tumor cells and were treated with the indicated doses of doxorubicin (0, 2.5 or 5 mg/kg; i.v.) on days 7 and 12 post-tumor cell injections. Spleens were collected and analyzed on day 17 and the proportion and absolute number of MDSC (CD11b+Gr-1+), the proportion of T lymphocytes (CD4+, CD8+) and NK cells (top panels), as well as the ratio of effector T or NK to suppressor MDSC (bottom panels) were determined. *P ≤ 0.05; **P ≤ 0.01; ***P ≤ 0.001. n=4 mice per group. Data represent one of 2 experiments performed and analyzed independently.

Supplemental Figure S6: Effects of doxorubicin on the suppressive function of residual MDSC. The immunosuppressive function of MDSC isolated from mice treated with the indicated doses of doxorubicin was assessed by determining their ability to impair CD4+ (left panels) or CD8+ (right panels) proliferation as explained in materials and methods. Representative Modfit analysis is shown.

Supplemental Figure S7: Effects of doxorubicin on MDSC expression of immunosuppressive factors and on MDSC differentiation.

Tumor-bearing mice were treated with doxorubicin (2.5 and 5 mg/kg) and spleens were collected and analyzed on day 17 post-tumor cell injection. A, Representative flow cytometry analysis of CD39 and CD73 expression by gated MDSC (CD11b+Gr-1+) in mice treated with the indicated doses of doxorubicin. B, Immunoblot analysis of p-Stat3, Stat3, S100A9 and S100A9 in MDSC isolated from mice treated with the indicated doses of doxorubicin. C, Representative flow cytometry analysis of the expression of CD206 (Mannose Receptor) and CCR7 by gated MDSC in mice treated with the indicated doses of doxorubicin. n=4 mice per group. Three independent experiments were performed.

Supplemental Figure S8:

A, Characterization of in vitro generated Th1 and Th17 lymphocytes. Th1 and Th17 were generated from naïve CD4+CD25-CD62L+ T cells. A, Real time PCR analysis of IFNγ and IL-17 in Th1 or Th17 cells. B, Measurement of IFNγ and IL-17 production in the culture supernatant of Th1 and Th17 lymphocytes using ELISA. C, Effects of doxorubicin plus Th1 or Th17 therapy on 4T1 tumor growth. Mice were injected orthotopically (mammary fat pad) with 4T1 tumor cells (1×106). Doxorubicin (5 mg/kg) was injected intravenously on day 7 and 12 post-tumor cell injection. Th1 or Th17 lymphocytes were administered on day 9 and 14 post-tumor cell injection, intravenously (1×106) and intratumoraly (2×106). Tumors were measured every other day and the tumor volume was determined by the formula (V=1/2(L×w2)); L, length (longest dimension); w, width (shortest dimension). ***$P \leq 0.001$. n=8 mice per group. Data represent one of 2 experiments performed and analyzed independently.

Supplemental Figure S1

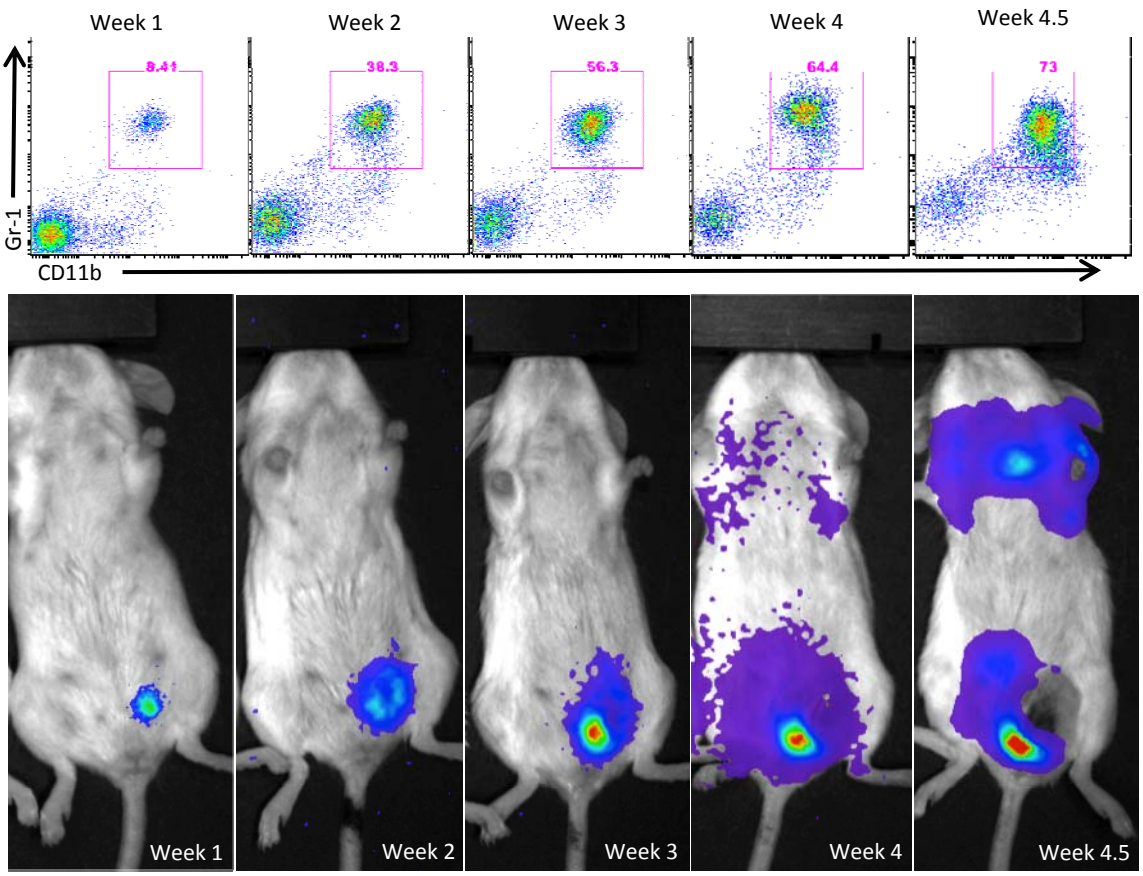

Supplemental Figure S2

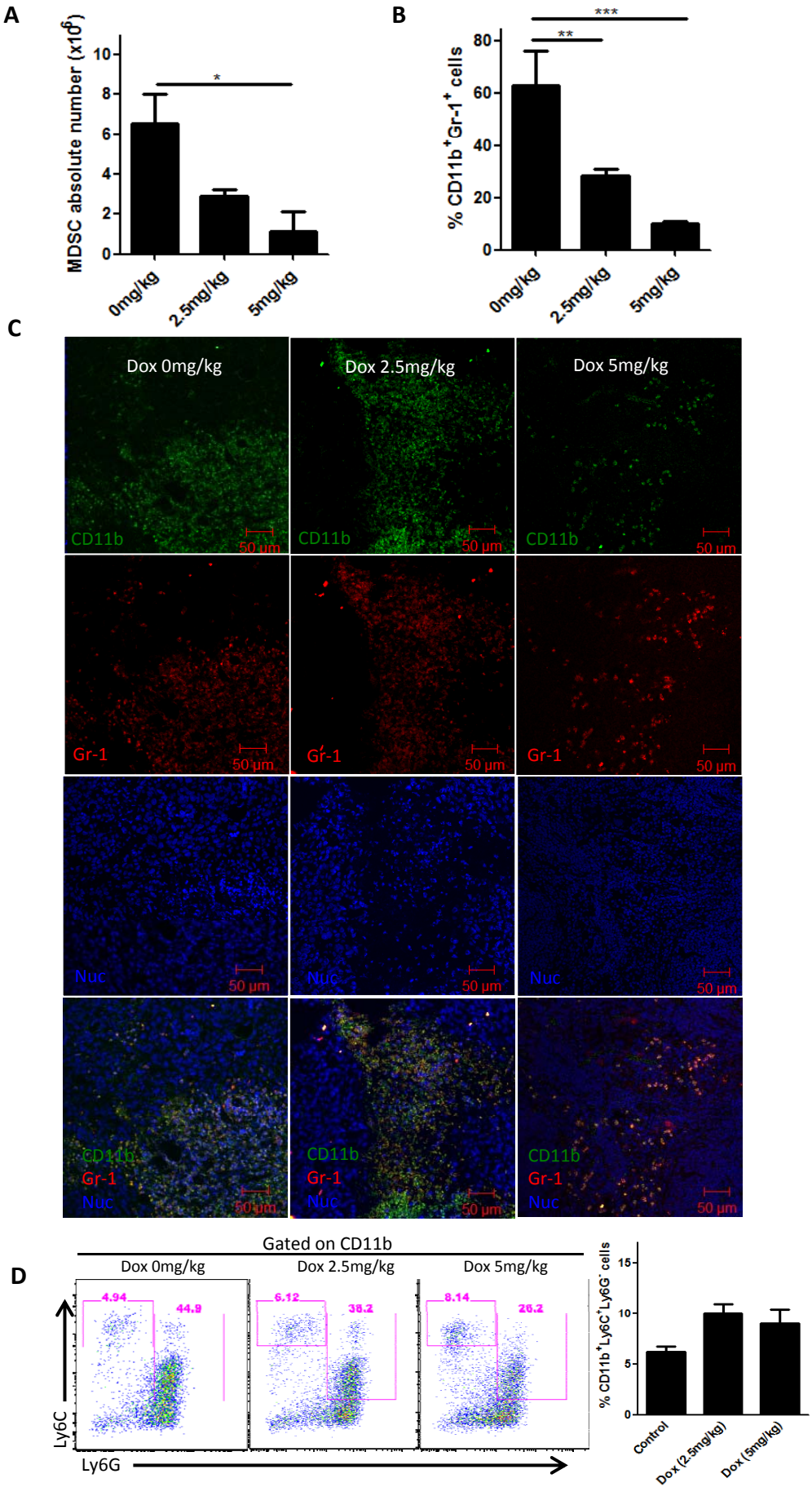

Supplemental Figure S3

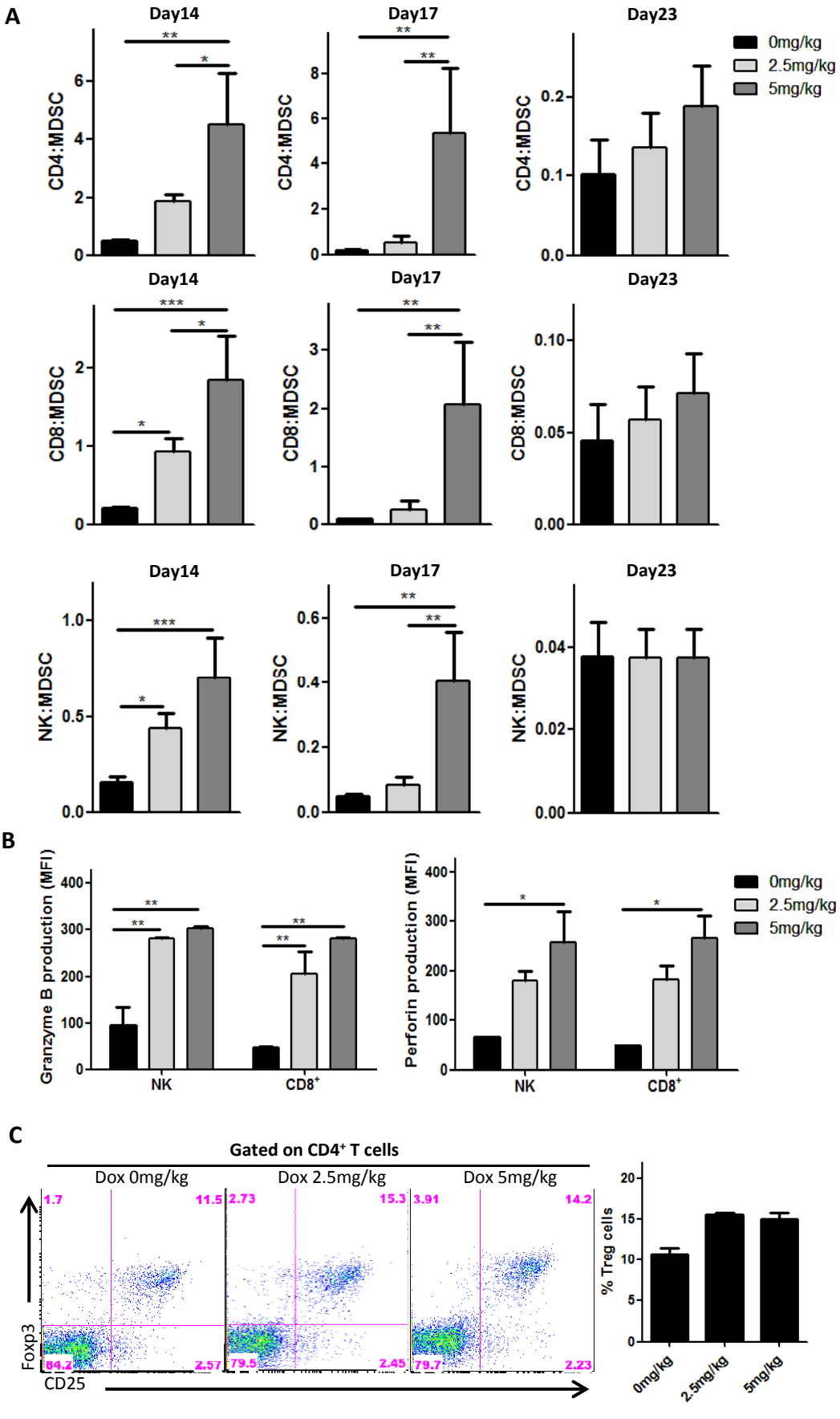

Supplemental Figure S4

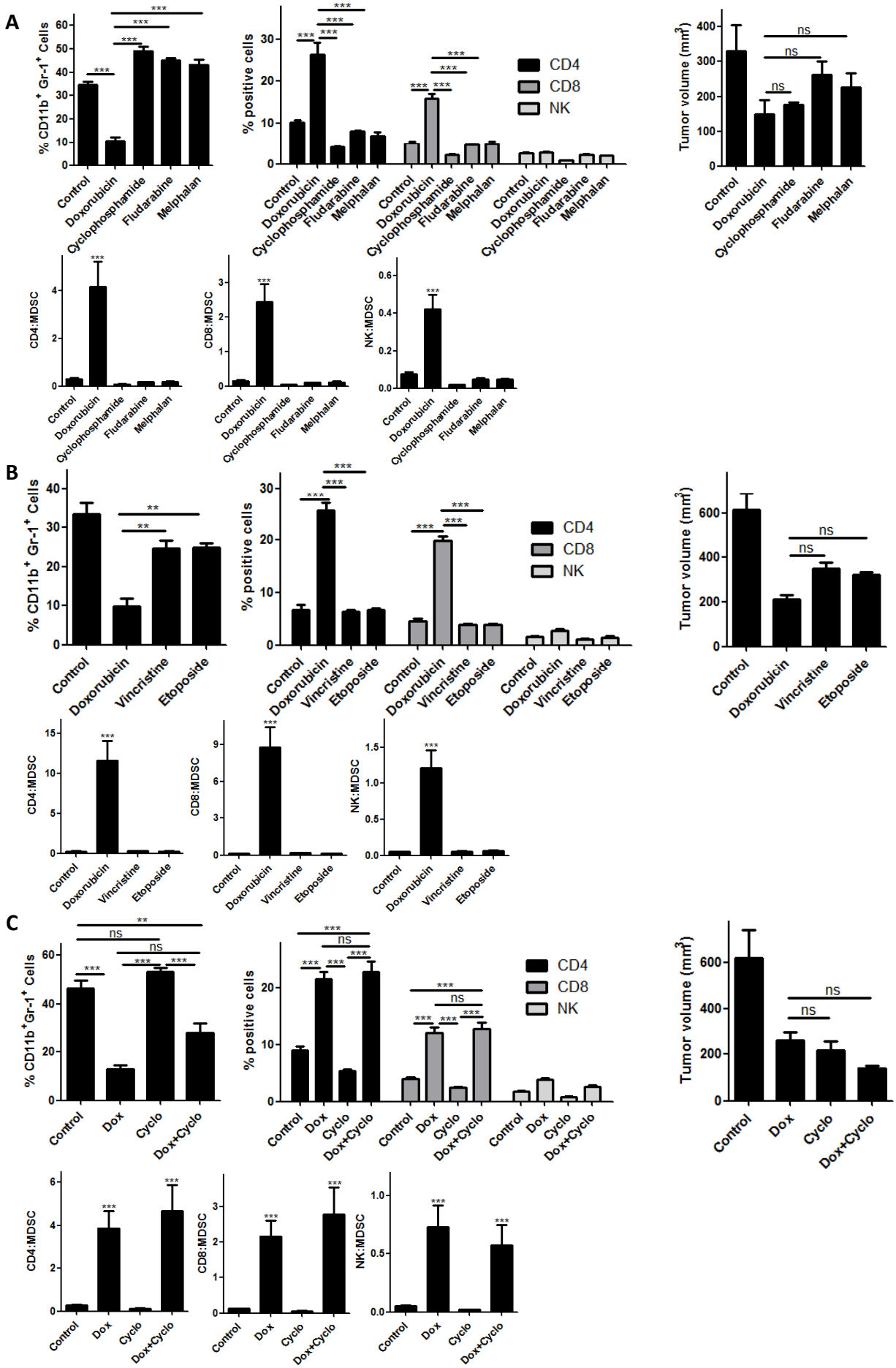

Supplemental Figure S5

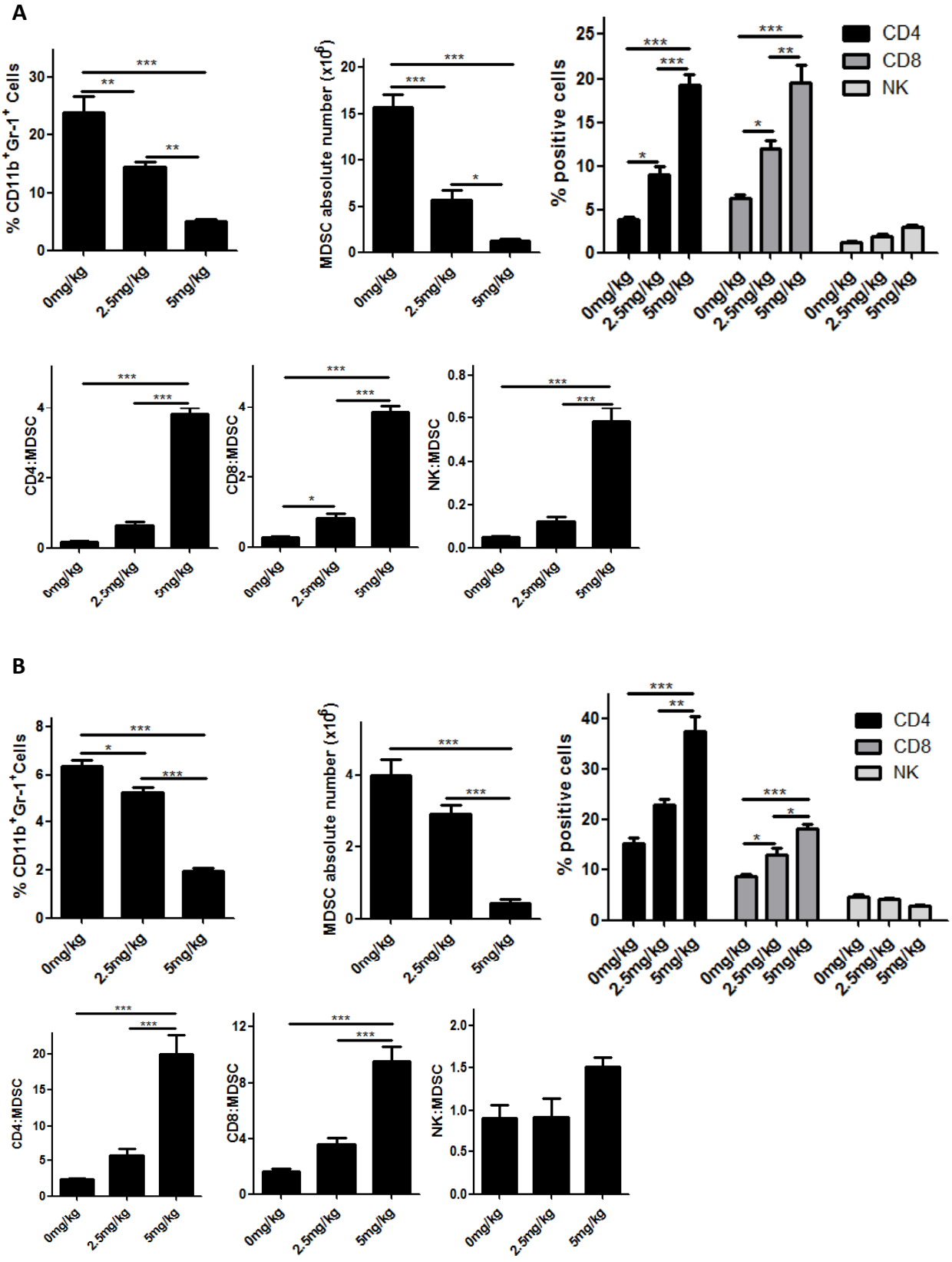

Supplemental Figure S6

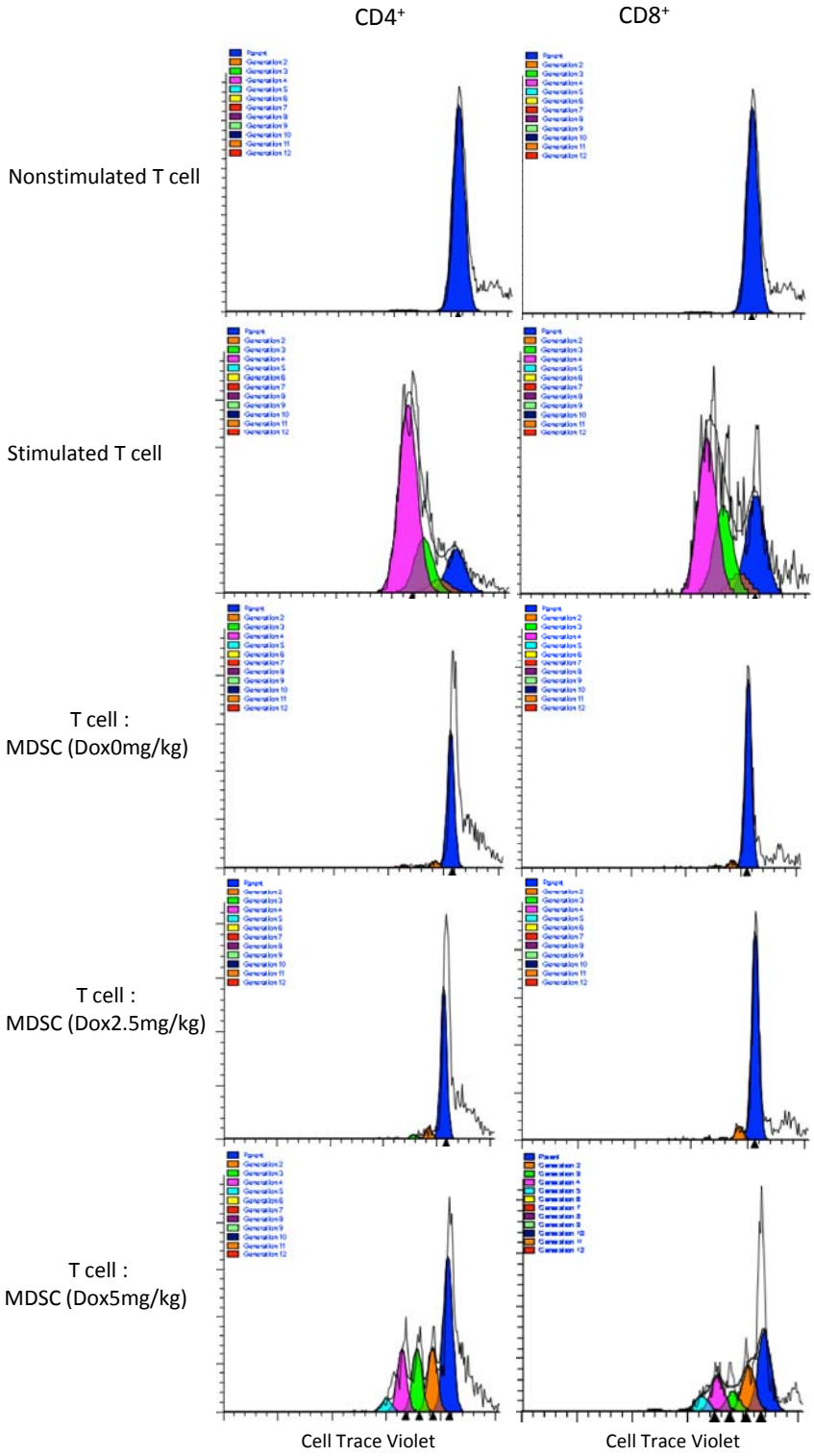

Supplemental Figure S7

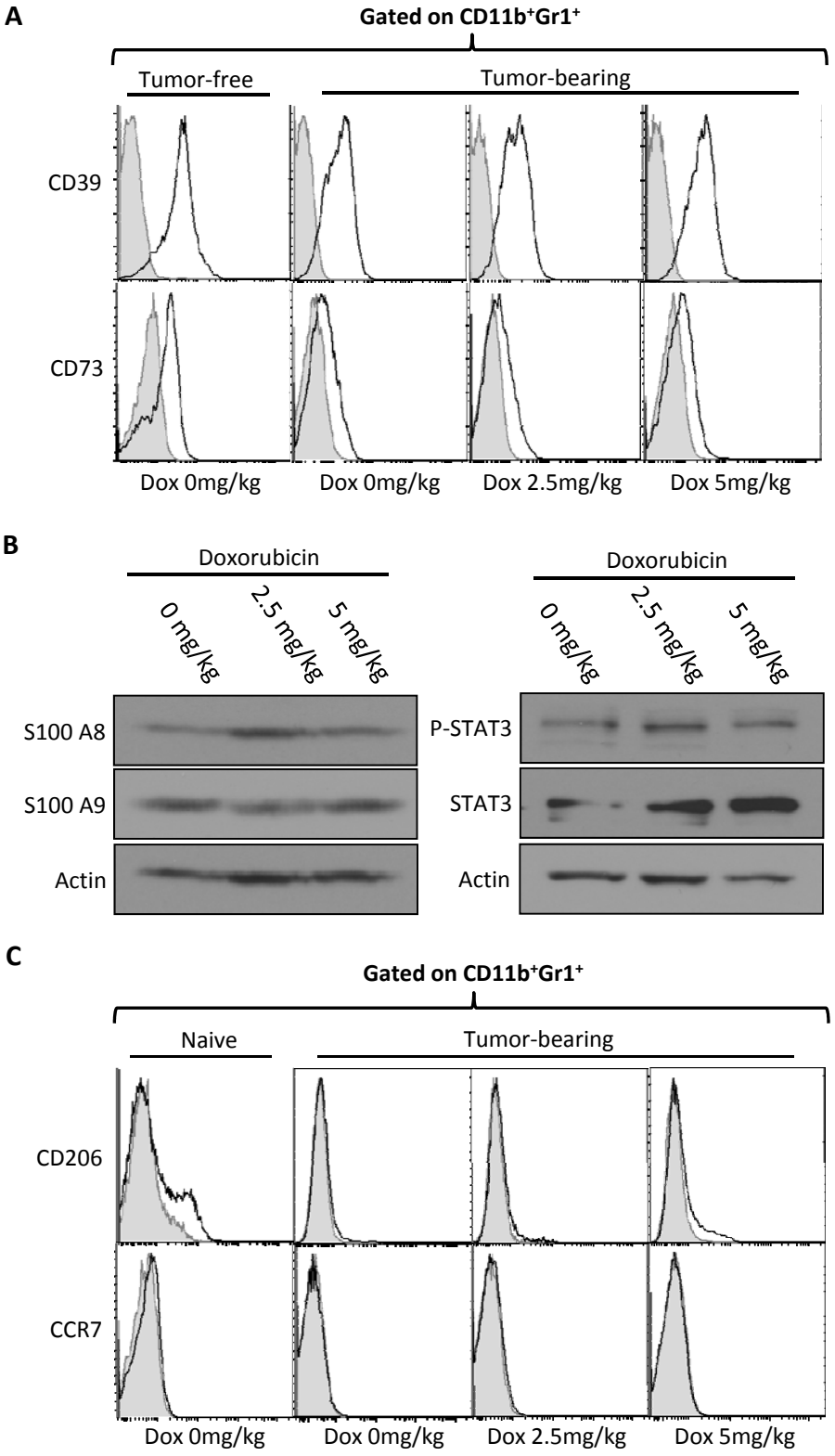

Supplemental Figure S8